Electronic Supplementary Material (ESI) for Chemical Communications.
This journal is © The Royal Society of Chemistry 2018

Electronic Supplementary Information

A planarized *B*-phenyldibenzoborepin: Impact of the structural constraint on its electronic properties and Lewis acidity.

Naoki Ando, Tomokatsu Kushida, and Shigehiro Yamaguchi*

Department of Chemistry, Graduate School of Science and Institute of Transformative Bio-Molecules (WPI-ITbM), Nagoya University, Furo, Chikusa, Nagoya 464-8602, Japan

E-mail: yamaguchi@chem.nagoya-u.ac.jp

Contents

1. Experimental Details

General Procedures. Melting points (mp) or decomposition temperatures were determined with a Yanaco MP-S3 instrument. ^{1}H, $^{13}C\{^{1}H\}$, and $^{11}B\{^{1}H\}$ NMR spectra were recorded with a JEOL AL-400 spectrometer in $CDCl_3$, C_6D_6, acetone-d_6, and pyridine-d_5 (400 MHz for ^{1}H, 100 MHz for ^{13}C, and 128 MHz for ^{11}B). The chemical shifts in ^{1}H NMR spectra are reported in δ ppm using the residual proton of the solvents, $CHCl_3$ (δ 7.26) in $CDCl_3$, $(CH_3)_2CO$ in acetone-d_6 (δ 2.05), and C_5H_5N in pyridine-d_5 (δ 7.58) as an internal standard and those in ^{13}C NMR spectra are reported using the solvent signals of $CDCl_3$ (δ 77.16), C_6D_6 (δ 128.06), and acetone-d_6 (δ 29.84) as an internal standard. The chemical shifts in ^{11}B NMR are reported using $BF_3{\cdot}OEt_2$ (δ 0.00) as an external standard. Mass spectra were measured with a Bruker micrOTOF Focus spectrometry system with the ionization method of APCI. Thin layer chromatography (TLC) was performed on plates coated with 0.25 mm thickness of silica gel $60F_{254}$ (Merck). Column chromatography was performed using PSQ100B (Fuji Silysia Chemicals). Recycling preparative HPLC was performed using LC-forte/R equipped with silica gel columns (YMC–Actus SIL, YMC) or LC-9201 (Japan Analytical Industry) equipped with silica gel column (Wakosil-II 5SIL-Prep, Wako). Recycling preparative gel permeation chromatography (GPC) was performed using LC-918 equipped with polystyrene gel columns (JAIGEL 1H and 2H, Japan Analytical Industry) using chloroform as an eluent. Anhydrous Et_2O and hexane were purchased from Kanto Chemicals and further purified by Glass Contour Solvent Systems. 2-Bromo-1,3-di(propen-2-yl)benzene,[1] 5-bromo-2-iodo-1,3-di(propen-2-yl)benzene,[2] and (*Z*)-1,2-bis(2-bromophenyl)ethene,[3] and dimethyl (2,4,6-triispropylphenyl)boronate[4] were prepared according to the literature methods. All reactions were carried out under a nitrogen atmosphere.

Scheme S1

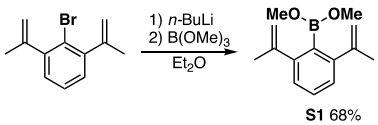

S1 68%

Dimethyl [2,6-di(propen-2-yl)phenyl]boronate (S1). To a solution of 2-bromo-1,3-di(propen-2-yl)benzene (488 mg, 2.06 mmol) in anhydrous Et_2O (5.0 mL) was added a hexane solution of *n*-BuLi (1.6 M, 1.40 mL, 2.24 mmol) dropwise at 0 °C. After stirring at the same temperature for 2 h, the resulting mixture was added to a solution of $B(OMe)_3$ (0.69 mL, 6.19 mmol) in anhydrous Et_2O (5.0 mL) at 0 °C. After stirring at the same temperature for 2 h, the resulting mixture was warmed to

room temperature and filtered through a pad of Celite® and concentrated under reduced pressure. The crude product was purified by silica gel column chromatography (2/1 hexane/CH_2Cl_2, R_f = 0.34) to give 320 mg (1.39 mmol) of **S1** in 68% yield as a colorless oil: ^{1}H NMR (400 MHz, acetone-d_6) δ 7.27–7.31 (m, 1H), 7.19–7.21 (m, 2H), 5.07–5.08 (m, 2H), 4.90–4.91 (m, 2H), 3.45 (s, 6H), 2.12 (dd, J_{HH} = 1.5 Hz, J_{HH} = 0.7 Hz, 6H); ^{13}C NMR (100 MHz, acetone-d_6) δ 148.5, 147.5, 128.6, 125.9, 114.1, 52.0, 24.1, a signal for the carbon atom bound to the boron atom were not observed due to the quadrupolar relaxation; ^{11}B NMR (128 MHz, acetone-d_6) δ 30.0; HRMS (APCI) *m*/*z* calcd for $C_{14}H_{19}{}^{11}BO_2$ $[M]^+$ 230.1473, found: 230.1474.

Scheme S2

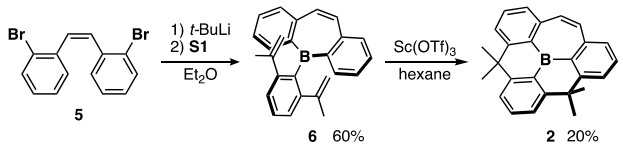

5-[2,6-Di(propen-2-yl)phenyl]-5*H*-dibenzo[*b*,*f*]borepin (6). To a solution of (*Z*)-1,2-bis(2-bromophenyl)ethene (**5)** (673 mg, 1.99 mmol) in anhydrous Et_2O (100 mL) was added a pentane solution of *t*-BuLi (1.62 M, 4.93 mL, 7.99 mmol) dropwise at –78 °C. After stirring at the same temperature for 3 h, a solution of **S1** (495 mg, 2.15 mmol) in anhydrous Et_2O (10 mL) was added to the mixture at the same temperature. The resulting mixture was warmed to room temperature and stirred under reflux conditions for 13 h. After a saturated NH_4Cl aqueous solution was added, the organic layer was separated and the aqueous layer was extracted with ethyl acetate three times. The combined organic layer was washed with brine, dried over $MgSO_4$, filtered, and concentrated under reduced pressure. The crude product was subjected to silica gel column chromatography (3/1 hexane/CH_2Cl_2, R_f = 0.56) and further purified by recrystallization from hexane to give 411 mg (1.19 mmol) of **6** in 60% yield as white solids: mp 138.5–139.2 °C; ^{1}H NMR (400 MHz, $CDCl_3$) δ 7.99 (dd, J_{HH} = 7.6 Hz, J_{HH} = 1.2 Hz, 2H), 7.67 (dd, J_{HH} = 7.6 Hz, J_{HH} = 1.2 Hz, 2H), 7.60 (td, J_{HH} = 7.2 Hz, J_{HH} = 1.6 Hz, 2H), 7.41–7.45 (m, 1H), 7.31–7.35 (m, 4H), 7.18 (s, 2H), 4.68 (m, 2H), 4.44 (s, 2H), 1.76 (s, 6H); ^{13}C NMR (100 MHz, $CDCl_3$) δ 147.4, 145.8, 143.1, 141.5, 133.9, 132.7, 131.7, 126.9, 126.7, 125.7, 112.0, 24.5, two signals for the carbon atoms bound to the boron atom were not observed due to the quadrupolar relaxation; ^{11}B NMR (128 MHz, $CDCl_3$) δ 61.3; HRMS (APCI) *m*/*z* calcd for $C_{26}H_{24}{}^{11}B$ $[M+H]^+$ 347.1966, found: 347.1951

Planarized *B*-phenyldibenzo[*b,f*]borepin 2. A mixture of **6** (174 mg, 0.50 mmol) and $Sc(OTf)_3$ (243 mg, 0.49 mmol) in anhydrous hexane (50 mL) was refluxed with stirring for 42 h. After cooling to room temperature, water was added to the mixture. The organic layer was separated, and the aqueous layer was extracted with ethyl acetate three times. The combined organic layer was washed with brine, dried over $MgSO_4$, filtered, and concentrated under reduced pressure. The crude product was subjected to silica gel column chromatography (5/1 hexane/CH_2Cl_2, R_f = 0.46) and further purified by recycling preparative HPLC to give 34.7 mg (0.10 mmol) of **2** in 20% yield as pale yellow solids: mp 173.4–174.1 °C; ^{1}H NMR (400 MHz, $CDCl_3$) δ 7.89 (dd, J_{HH} = 8.0 Hz, J_{HH} = 1.2 Hz, 2H), 7.72 (t, J_{HH} = 7.6 Hz, 2H), 7.61–7.67 (m, 4H), 7.53–7.57 (m, 1H), 7.21 (s, 2H), 1.77 (s, 12H) ; ^{13}C NMR (100 MHz, C_6D_6) δ, 160.3, 156.3, 145.9, 134.5, 131.8, 131.7, 131.6, 125.2, 123.2, 43.4, 36.2, two signals for the carbon atoms bound to the boron atom were not observed due to the quadrupolar relaxation; ^{11}B NMR (128 MHz, $CDCl_3$) δ 46.2; HRMS (APCI) *m*/*z* calcd for $C_{26}H_{24}{}^{11}B$ $[M+H]^+$ 347.1966, found: 347.1964.

Scheme S3

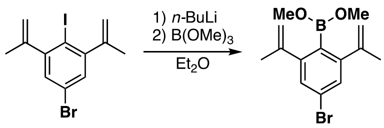

S2 45%

Dimethyl [4-bromo-2,6-di(propen-2-yl)phenyl]boronate (S2). To a solution of 5-bromo-2-iodo-1,3-di(propen-2-yl)benzene (1.09 g, 3.00 mmol) in anhydrous Et_2O (15 mL) was added a hexane solution of *n*-BuLi (1.6 M, 2.00 mL, 3.20 mmol) dropwise at –78 °C. After stirring at the same temperature for 2 h, a solution of $B(OMe)_3$ (1.00 mL, 9.00 mmol) in anhydrous Et_2O (4.5 mL) was added to the mixture at –78 °C. After stirring at the same temperature for 1 h, the resulting mixture was warmed to room temperature and filtered through a pad of Celite® and concentrated under reduced pressure. The crude product was purified by silica gel column chromatography (2/1 hexane/CH_2Cl_2, R_f = 0.35) to give 422 mg (1.36 mmol) of **S2** in 45% yield as a colorless oil: ^{1}H NMR (400 MHz, $CDCl_3$) δ 7.31 (s, 2H), 5.10–5.11 (m, 2H), 4.96 (s, 2H), 3.48 (s, 6H), 2.11 (s, 6H); ^{13}C NMR (100 MHz, $CDCl_3$) δ □□□, a signal for the carbon atom bound to the boron atom were not observed due to the quadrupolar relaxation; ^{11}B NMR (128 MHz, $CDCl_3$) δ □□□□; HRMS (APCI) *m*/*z* calcd for $C_{14}H_{19}{}^{11}B^{79}BrO_2$ $[M+H]^+$ 309.0656, found: 309.0663.

Scheme S4

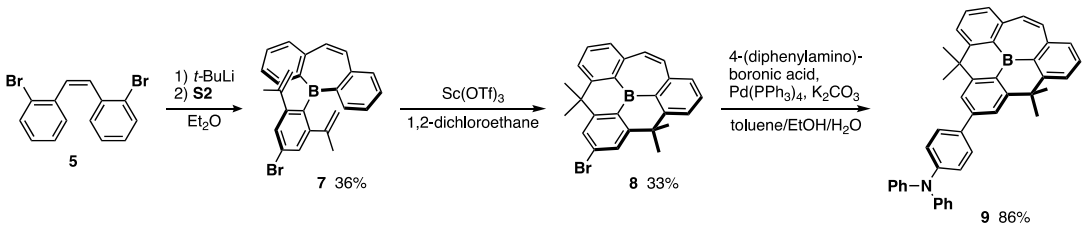

5-[4-Bromo-2,6-di(propen-2-yl)phenyl]-5*H*-dibenzo[*b*,*f*]borepin (7). To a solution of (*Z*)-1,2-bis(2-bromophenyl)ethene (439 mg, 1.30 mmol) in anhydrous Et_2O (65 mL) was added a pentane solution of *t*-BuLi (1.62 M, 3.20 mL, 5.18 mmol) dropwise at –78 °C. After stirring at the same temperature for 2 h, a solution of **S2** (408 mg, 1.32 mmol) in anhydrous Et_2O (5.0 mL) was added to the mixture at the same temperature. The resulting mixture was warmed to room temperature and stirred under reflux condition for 16 h. Then a saturated NH_4Cl aqueous solution was added. The organic layer was separated and the aqueous layer was extracted with ethyl acetate three times. The combined organic layer was washed with brine, dried over $MgSO_4$, filtered, and concentrated under reduced pressure. The crude product was subjected to silica gel column chromatography (5/1 hexane/CH_2Cl_2, R_f = 0.44) and further purified by recrystallization from hexane to give 199 mg (0.47 mmol) of **7** in 36% yield as white solids: mp 147.8–148.6 °C; ^{1}H NMR (400 MHz, $CDCl_3$) δ 7.96 (d, J_{HH} = 7.6 Hz 2H), 7.69 (d, J_{HH} = 7.2 Hz, 2H), 7.62 (td, J_{HH} = 7.2 Hz, J_{HH} = 1.2 Hz, 2H), 7.46 (s, 2H), 7.35 (td, J_{HH} = 7.6 Hz, J_{HH} = 1.2 Hz, 2H), 7.19 (s, 2H), 4.69 (s, 2H), 4.45 (s, 2H), 1.72 (s, 6H); ^{13}C NMR (100 MHz, $CDCl_3$) δ 147.7, 146.1, 143.3, 141.4, 133.9, 132.9, 132.0, 128.6, 126.8, 121.2, 118.9, 24.4, two signals for the carbon atoms bound to the boron atom were not observed due to the quadrupolar relaxation; ^{11}B NMR (128 MHz, $CDCl_3$) δ 61.7; HRMS (APCI) *m*/*z* calcd for $C_{26}H_{22}{}^{11}B^{79}Br$ $[M]^+$ 424.0992, found: 424.0999.

Bromo-substituted planarized *B*-phenyldibenzo[*b*,*f*]borepin 8. A mixture of **7** (98.9 mg, 0.23 mmol) and $Sc(OTf)_3$ (116 mg, 0.24 mmol) in 1,2-dichloroethane (120 mL) was stirred under reflux conditions. After stirring for 17 h, another amount of $Sc(OTf)_3$ (50.0 mg, 0.10 mmol) was added to the mixture and stirred for additional 7 h. After cooling to room temperature, the reaction mixture was filtered through a pad of SiO_2 and concentrated under reduced pressure. The crude product was subjected to silica gel column chromatography (20/1 hexane/CH_2Cl_2, R_f = 0.19) and further purified by recycling preparative HPLC (5/1 hexane/CH_2Cl_2, R_f = 0.50) to give 32.3 mg (0.08 mmol) of **7** in

33% yield as yellow solids: mp. 125.6–126.5 °C; ^{1}H NMR (400 MHz, $CDCl_3$) δ 7.87 (dd, J_{HH} = 8.0 Hz, J_{HH} = 1.2 Hz, 2H), 7.78 (s, 2H), 7.73 (t, J_{HH} = 7.6 Hz, 2H), 7.64 (dd, J_{HH} = 8.0 Hz, J_{HH} = 1.2 Hz, 2H), 7.22 (s, 2H), 1.76 (s, 12H) ; ^{13}C NMR (100 MHz, $CDCl_3$) δ 159.3, 158.2, 145.4, 134.1, 131.9, 131.6, 126.8, 126.2, 125.0, 43.4, 36.1, two signals for the carbon atoms bound to the boron atom were not observed due to the quadrupolar relaxation; ^{11}B NMR (128 MHz, $CDCl_3$) δ 46.1; HRMS (APCI) *m*/*z* calcd for $C_{26}H_{22}{}^{11}B^{79}Br$ $[M]^+$ 424.0992, found: 424.1007.

4-(*N*,*N*-diphenylamino)phenyl-substituted planarized *B*-phenyldibenzo[*b*,*f*]borepin 9. A mixture of **8** (68.5 mg, 0.16 mmol), 4-(*N*,*N*-diphenylamino)phenylboronic acid (51.3 mg, 0.18 mmol), $Pd(PPh_3)_4$ (9.7 mg, 8.4 μmol), and K_2CO_3 (45.7 mg, 0.33 mmol) in degassed toluene (1.0 mL)/EtOH (1.0 mL)/H_2O (0.5 mL) was refluxed with stirring for 11 h. After cooling to room temperature, a saturated NH_4Cl aqueous solution was added. The organic layer was separated and the aqueous layer was extracted with CH_2Cl_2 three times. The combined organic layer was washed with brine, dried over $MgSO_4$, filtered, and concentrated under reduced pressure. The crude product was subjected to silica gel column chromatography (1/1 hexane/CH_2Cl_2, R_f = 0.65) and further purified by recycling preparative GPC ($CHCl_3$) to give 81.5 mg (0.14 mmol) of **9** in 86% yield as yellow solids: mp. 224.4–225.4 °C; ^{1}H NMR (400 MHz, $CDCl_3$) δ 7.91 (d, J_{HH} = 7.6 Hz, 2H), 7.84 (s, 2H), 7.72 (t, J_{HH} = 7.6 Hz, 2H), 7.61–7.64 (m, 4H), 7.30 (t, J_{HH} = 6.8 Hz, 4H), 7.17–7.22 (m, 8H), 7.06 (t, J_{HH} = 7.6 Hz, 2H), 1.83 (s, 12H); ^{13}C NMR (100 MHz, $CDCl_3$) δ 159.9, 156.6, 147.8, 147.7, 145.3, 143.1, 135.8, 134.1, 131.6, 131.4, 129.5, 128.3, 125.1, 124.7, 123.9, 123.2, 121.5, 43.5, 36.2, two signals for the carbon atoms bound to the boron atom were not observed due to the quadrupolar relaxation; ^{11}B NMR (128 MHz, $CDCl_3$) δ 46.6; HRMS (APCI) *m*/*z* calcd for $C_{44}H_{37}{}^{11}BN$ $[M+H]^+$ 590.3014, found: 590.3029.

Scheme S5

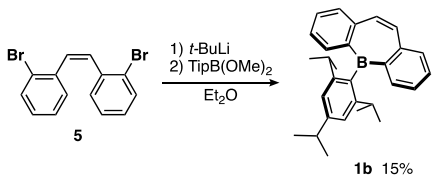

5-(2,4,6-Triisopropylphenyl)-5*H*-dibenzo[*b*,*f*]borepin (1b). To a solution of (*Z*)-1,2-bis(2-bromophenyl)ethene (**5**) (338 mg, 1.00 mmol) in anhydrous Et_2O (50 mL) was added a pentane solution of *t*-BuLi (1.62 M, 2.47 mL, 4.00 mmol) dropwise at –78 °C. After stirring at the same

temperature for 2 h, a solution of $TipB(OMe)_2$ (282 mg, 1.02 mmol) in anhydrous Et_2O (5.0 mL) was added to the mixture at the same temperature. The resulting mixture was warmed to room temperature and stirred under reflux conditions for 17 h. After a saturated NH_4Cl aqueous solution was added, the organic layer was separated and the aqueous layer was extracted with Et_2O three times. The combined organic layer was washed with brine, dried over $MgSO_4$, filtered, and concentrated under reduced pressure. The crude product was subjected to silica gel column chromatography (10/1 hexane/CH_2Cl_2, R_f = 0.60) and further purified by recrystallization from EtOH to give 59.7 mg (0.15 mmol) of **1b** in 15% yield as white solids: mp 201.7 °C (dec.); ^{1}H NMR (400 MHz, $CDCl_3$) δ 8.10 (dd, J_{HH} = 7.6 Hz, J_{HH} = 1.6 Hz, 2H), 7.79 (dd, J_{HH} = 8.0 Hz, J_{HH} = 1.2 Hz, 2H), 7.70 (td, J_{HH} = 7.6 Hz, J_{HH} = 1.6 Hz, 2H), 7.41 (td, J_{HH} = 7.6 Hz, J_{HH} = 1.2 Hz, 2H), 7.33 (s, 2H), 7.06 (s, 2H), 3.01 (sep, J_{HH} = 6.8 Hz, 1H), 2.22 (sep, J_{HH} = 6.8 Hz, 2H), 1.38 (d, J_{HH} = 6.8 Hz, 6H), 0.93 (d, J_{HH} = 6.8 Hz, 12H); ^{13}C NMR (100 MHz, $CDCl_3$) δ 149.0, 148.1, 143.8, 143.1, 134.2, 133.0, 132.7, 126.7, 120.3, 35.6, 34.3, 24.4, 24.2, two signals for the carbon atoms bound to the boron atom were not observed due to the quadrupolar relaxation; ^{11}B NMR (128 MHz, $CDCl_3$) δ 64.8; HRMS (APCI) *m*/*z* calcd for $C_{29}H_{33}{}^{11}B$ $[M]^+$ 392.2670, found: 392.2660.

2. X-ray Crystallographic Analysis

Structural analysis of 2. Block-shaped yellow single crystals of **2** were obtained by vapor diffusion of acetonitrile into an ethyl acetate solution of **2**. The intensity data were collected at 123 K on a Rigaku Single Crystal X-ray diffractometer equipped with FR-X generator, Varimax optics, and PILATUS 200K photon counting detector with MoKα radiation (λ = 0.71075 Å). A total of 23539 reflections were measured with the maximum 2θ angle of 50°, of which 3210 were independent reflections (R_{int} = 0.0190). The structure was solved by direct methods (SHELXS) and refined by the full-matrix least-squares on F^2 (SHELXL-2017/1).[5] All non-hydrogen atoms were refined anisotropically and all hydrogen atoms were placed using AFIX instructions. The crystal data are as follows: $C_{26}H_{23}B$; FW = 346.25, crystal size 0.30 × 0.30 × 0.25 mm^3, trigonal, *R*–3, *a* = 33.652(8) Å, *b* = 33.652(8) Å, *c* = 8.379(2) Å, *V* = 8218(5) Å^3, *Z* = 18, D_c = 1.259 g cm^{-3}, μ = 0.070 mm^{-1}, R_1 = 0.0338 ($I > 2\sigma(I)$), wR_2 = 0.0865 (all data), GOF = 1.036.

Structural analysis of 2·DMAP. Plate-shape colorless single crystals of **2**·DMAP were obtained by slow cooling a mixture of **2** and DMAP in hot toluene. The intensity data were collected at 123 K on a Rigaku Saturn CCD diffractometer with VariMax monochromator MoKα radiation (λ = 0.71075 Å). A total of 19899 reflections were measured at the maximum 2θ angle of 50°, of which 5349

were independent reflections (R_{int} = 0.0301). The structure was solved by direct methods (SHELXS) and refined by full-matrix least-squares procedures on F^2 for all reflections (SHELXL-2017/1).[5] All non-hydrogen atoms were refined anisotropically and all hydrogen atoms were placed using AFIX instructions. The crystal data are as follows: $C_{40}H_{41}BN_2$; FW = 560.56, crystal size 0.40 × 0.40 × 0.05 mm^3, monoclinic, $P2_1/n$, a = 13.674(2) Å, b = 16.498(3) Å, c = 14.380(2) Å, β = 108.3840(18)°, V = 3078.6(8) Å^3, Z = 4, D_c = 1.209 g cm^{-3}, μ = 0.069 mm^{-1}, R_1 = 0.0395 ($I > 2\sigma(I)$), wR_2 = 0.1059 (all data), GOF = 1.035.

Structural analysis of 9. Block-shaped yellow single crystals of **9** were obtained by vapor diffusion of acetonitrile into an ethyl acetate solution of **9**. The intensity data were collected at 123 K on a Rigaku Saturn CCD diffractometer with VariMax monochromator MoKα radiation (λ = 0.71075 Å). A total of 10265 reflections were measured at the maximum 2θ angle of 50°, of which 2784 were independent reflections (R_{int} = 0.0279). The structure was solved by direct methods (SHELXS) and refined by full-matrix least-squares procedures on $\boldsymbol{F}^2$ for all reflections (SHELXL-2017/1).[5] All non-hydrogen atoms were refined anisotropically and all hydrogen atoms were placed using AFIX instructions. The crystal data are as follows: $C_{44}H_{36}BN$; FW = 589.55, crystal size 0.40 × 0.40 × 0.20 mm^3, monoclinic, $P2/c$, a = 10.379(3) Å, b = 18.921(5) Å, c = 8.611(2) Å, β = 109.582(3)°, V = 1593.2(7) Å^3, Z = 2, D_c = 1.229 g cm^{-3}, μ = 0.070 mm^{-1}, R_1 = 0.0418 ($I > 2\sigma(I)$), wR_2 = 0.1042 (all data), GOF = 1.058.

Structural analysis of 1b. Plate-shaped colorless single crystals of **1b** were obtained by slow evaporation from a hexane solution of **1b**. The intensity data were collected at 123 K on a Rigaku Single Crystal X-ray diffractometer equipped with FR-X generator, Varimax optics, and PILATUS 200K photon counting detector with MoKα radiation (λ = 0.71075 Å). A total of 24128 reflections were measured with the maximum 2θ angle of 55°, of which 10526 were independent reflections (R_{int} = 0.0169). The structure was solved by direct methods (SHELXS) and refined by the full-matrix least-squares on F^2 (SHELXL-2017/1).[5] All non-hydrogen atoms were refined anisotropically and all hydrogen atoms were placed using AFIX instructions. The crystal data are as follows: $C_{29}H_{33}B$; FW = 392.36, crystal size 0.31 × 0.24 × 0.02 mm^3, triclinic, P–1, a = 8.7378(9) Å, b = 16.5639(17) Å, c = 16.8755(18) Å, α = 80.618(4)°, β = 84.316(4)°, γ = 79.857(3)°,V = 2365.9(4) Å^3, Z = 4, D_c = 1.102 g cm^{-3}, μ = 0.061 mm^{-1}, R_1 = 0.0402 ($I > 2\sigma(I)$), wR_2 = 0.1039 (all data), GOF = 1.013.

Crystallographic data of **2**, **2**·DMAP, **9**, and **1b** have been deposited in the Cambridge Crystallographic Data Centre as supplementary publication no. CCDC-1827102, 1827103, 1827104, and 1827105. The data can be obtained free of charge from the Cambridge Crystallographic Data Centre via www.ccdc.cam.ac.uk/data_request/cif.

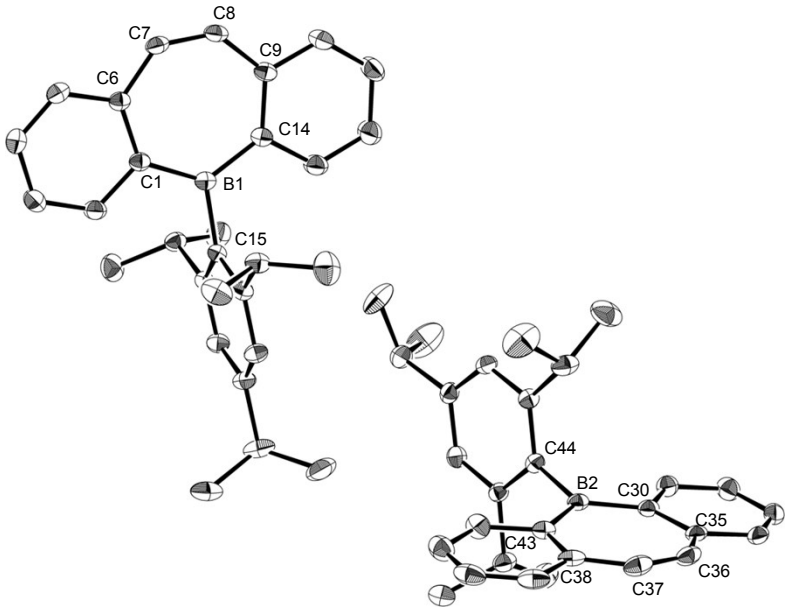

Figure S1. ORTEP drawing of **1b** (50% probability for thermal ellipsoids). Hydrogen atoms are omitted for clarity.

Table S1. Selected Bond Lengths (Å) and Angles (°) of **1b**

B1–C1	1.5606(16)	B2–C30	1.5585(17)
B1–C14	1.5611(17)	B2–C43	1.5630(17)
B1–C15	1.5957(16)	B2–C44	1.5967(16)
C1–C6	1.4256(15)	C30–C35	1.4257(15)
C6–C7	1.4516(16)	C35–C36	1.4481(17)
C7–C8	1.3424(17)	C36–C37	1.3441(19)
C8–C9	1.4530(16)	C37–C38	1.4519(18)
C9–C14	1.4217(15)	C38–C43	1.4225(16)
C1–B1–C14	127.04(10)	C30–B2–C43	126.96(10)
C1–B1–C15	117.17(10)	C30–B2–C44	117.86(10)
C14–B1–C15	115.79(10)	C43–B2–C44	115.18(10)

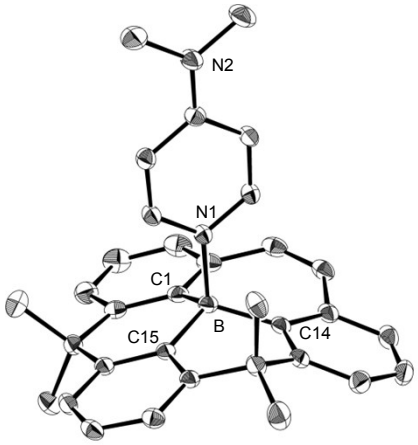

Figure S2. ORTEP drawing of **2**·DMAP (50% probability for thermal ellipsoids). Hydrogen atoms and solvents are omitted for clarity.

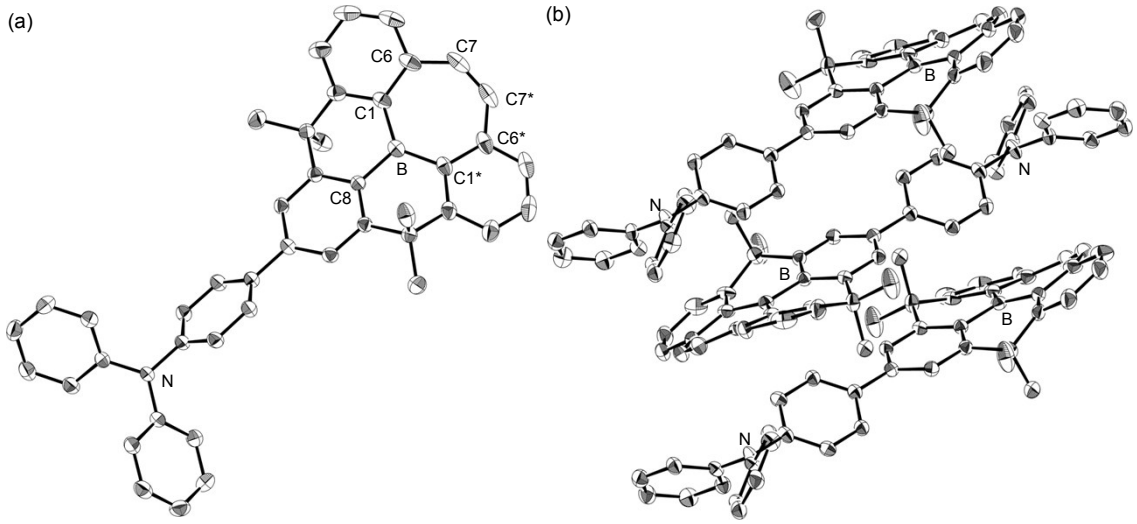

Figure S3. (a) ORTEP drawing of **9** (50% probability for thermal ellipsoids) and (b) the crystal packing of **9**. Hydrogen atoms are omitted for clarity.

3. Cyclic Voltammetry

Cyclic voltammetry (CV) was performed on an ALS/chi-617A electrochemical analyzer. The CV cell was consisted of a glassy carbon electrode, a Pt wire counter electrode, and an $Ag/AgNO_3$ reference electrode. The measurements were carried out under an argon atmosphere using a THF solution of sample with a concentration of 1 mM and 0.1 M tetrabutylammonium hexafluorophosphate (n-$Bu_4N^+PF_6^-$) as a supporting electrolyte. The redox potentials were calibrated with ferrocene as an internal standard.

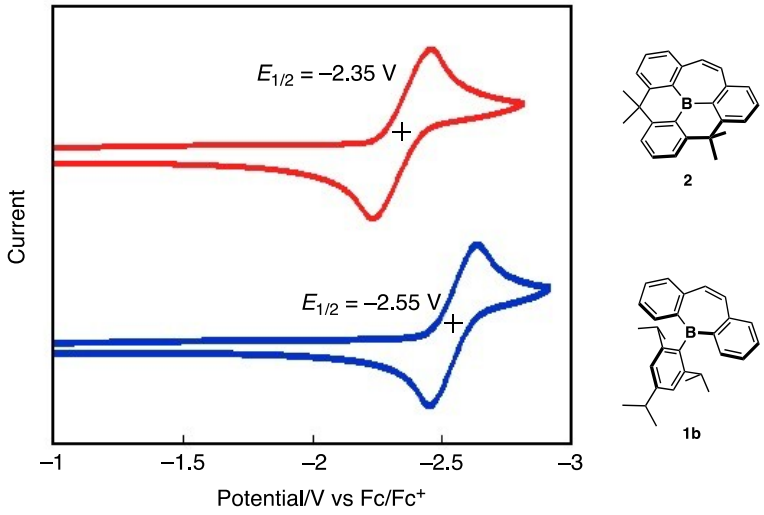

Figure S4 Cyclic voltammograms of **2** (top) and **1b** (bottom) in THF (1 mM), measured with n-$Bu_4N^+PF_6^-$ (0.1 M) as a supporting electrolyte at a scan rate of 100 mV s^{-1}.

4. Photophysical Properties

UV-vis absorption and fluorescence spectra were measured with a Shimadzu UV-3600 Plus spectrometer and a JASCO FP-8500 spectrofluorometer, respectively, using dilute sample solutions in a 1 cm square quartz cuvette. Fluorescence quantum yields were determined with a Hamamatsu Absolute PL Quantum Yield spectrometer C11347 and C9920-02 calibrated integrating sphere system. Fluorescence lifetime was measured with a Hamamatsu Picosecond fluorescence measurement system C4780.

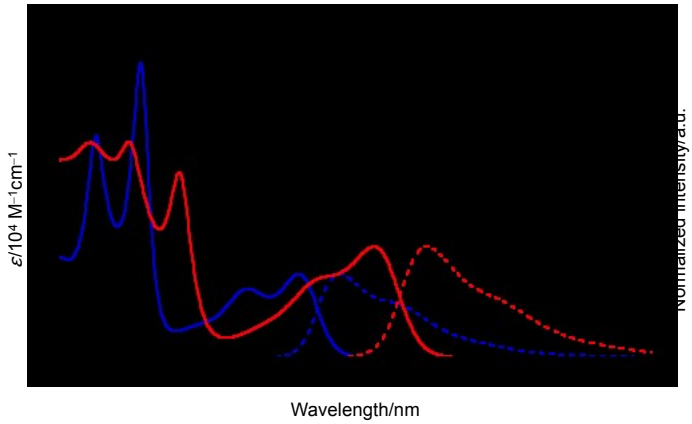

Figure S5. UV-vis absorption (solid lines) and fluorescence (dashed lines) spectra of 2 (red) and 1b (blue) in THF.

Table S2. Photophysical Data for **2** and **1b** in THF

Compd	λ_{abs} / nm (log ε)	λ_{em} / nm	Stokes shift / cm^{-1}	Φ_F[a]	τ / ns	k_r / 10^7 s^{-1}	k_{nr} / 10^7 s^{-1}
2	406 (3.93)	424	1050	0.64	8.7	7.8	3.8
1b	381 (3.80)	395	930	0.81	10.8	7.5	1.8

[a]Absolute fluorescence quantum yields determined by a calibrated integrating sphere system within ±3% error.

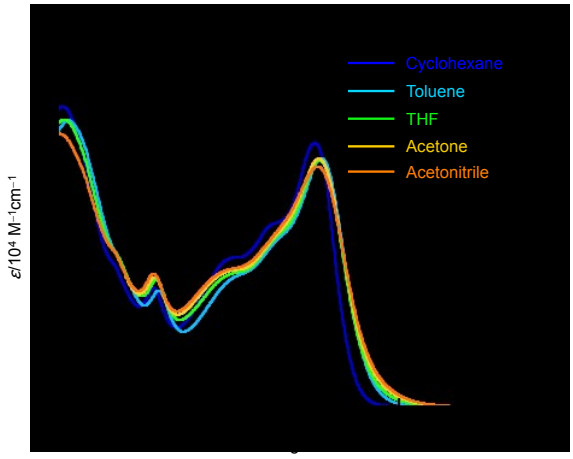

Figure S6. UV-vis absorption spectra of **9** in various solvents.

Table S3. Photophysical Data for **9** in Various Solvents

Solvent	λ_{abs} /nm	log ε	λ_{em} /nm	Stokes shift /cm^{-1}	Φ_F[a]	τ /ns	k_r /10^8 s^{-1}	k_{nr} /10^7 s^{-1}
Cyclohexane	413	4.56	434	1160	0.95	2.5	3.9	2.2
Toluene	416	4.53	461	2340	0.93	2.4	3.9	3.0
THF	415	4.53	512	4550	0.93	3.5	2.7	2.1
Acetone	415	4.53	556	6080	0.93	4.7	2.0	1.5
Acetonitrile	415	4.52	593	7270	0.91	5.7	1.6	1.6

[a]Absolute fluorescence quantum yields determined by a calibrated integrating sphere system within ±3% error.

5. UV-vis Absorption Titration Experiments with Pyridine

UV-vis absorption spectra were measured with a Shimadzu UV-3600 Plus spectrometer using dilute sample solutions in a 1 cm square quartz cuvette. The titration experiments were conducted according to the literature method.[6]

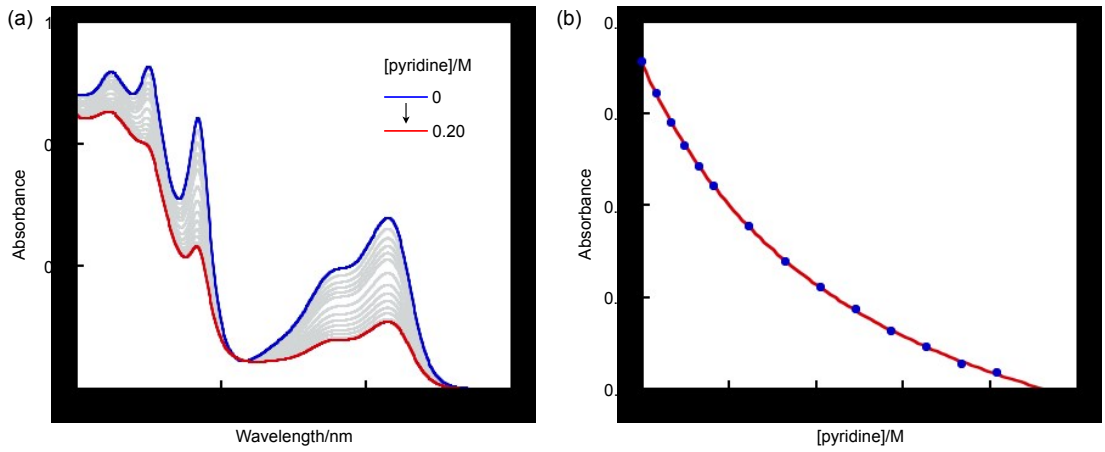

Figure S7. (a) UV-vis absorption spectral changes upon addition of pyridine to a toluene solution of **2** (6.0×10^{-5} M) and (b) plots of the absorbance at 408 nm with a fitting curve for the binding constant of **2** toward pyridine. The binding constant was estimated to be 7.7 M^{-1} (R^2 = 0.99984).

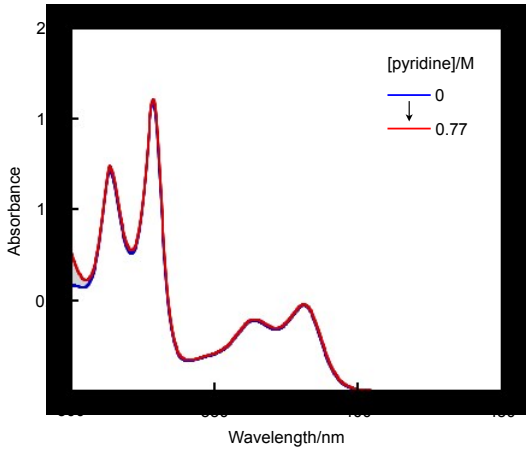

Figure S8. UV-vis absorption spectral changes upon addition of pyridine to a toluene solution of **1b** (7.3×10^{-5} M).

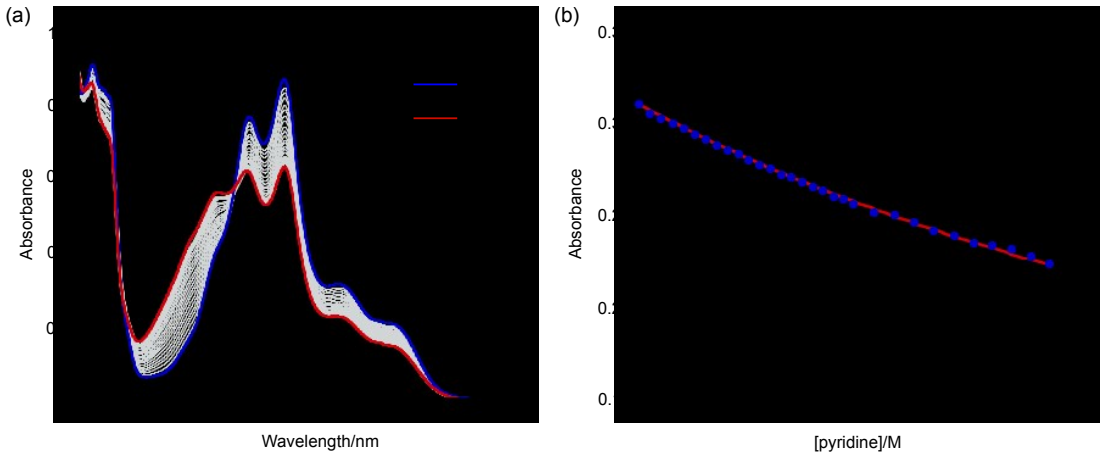

Figure S9. (a) UV-vis absorption spectral changes upon addition of pyridine to a toluene solution of **4** (5.3×10^{-5} M) and (b) plots of the absorbance at 620 nm with a fitting curve for the binding constant of **4** toward pyridine. The binding constant was estimated to be 0.35 M^{-1} ($R^2 = 0.9991$).

6. Theoretical Calculations

Geometry optimizations of **1b**, **2**, $\mathbf{10}_{\perp}$, and radical anion $\mathbf{2}^{\bullet-}$ were performed using the Gaussian 16 program[7] at the (U)B3PW91/6-31+G(d) level of theory. The structures optimized at the B3PW91/6-31+G(d) level of theory were employed for the TD-DFT calculations at the B3LYP/6-31+G(d) level of theory. The model geometry of $\mathbf{10}_{//}$with the fixed dihedral angle of 0° was derived from the optimized geometry of $\mathbf{10}_{\perp}$, where all other structural parameters calculated for $\mathbf{10}_{\perp}$ remained constant, and calculated at single-point at the B3LYP/6-31+G(d) level of theory.[8] The Cartesian

coordinates of the optimized geometries of **1b**, **2**, $\mathbf{10}_{\perp}$, and radical anion $\mathbf{2}^{\bullet-}$ are shown in Tables S4–S9.

Table S4. Cartesian Coordinates of **p-2**

atom	*x*	*y*	*z*	atom	*x*	*y*	*z*
B	-0.38986213	-0.05623699	0.00000000	H	3.86872074	-0.21808169	2.12461960
C	-1.08313558	-0.03290111	1.41665398	H	3.86872074	-0.21808169	-2.12461960
C	-2.20353000	0.21878435	4.05183676	H	5.08996845	-0.35122440	0.00000000
C	-0.26273159	0.09808153	2.57677879	C	-3.53374771	-0.30603806	0.67373484
C	-2.49832001	-0.09753637	1.65924598	H	-4.51697067	-0.46189337	1.11669748
C	-3.02422187	0.02146763	2.96060323	C	-3.53374771	-0.30603806	-0.67373484
C	-0.83213987	0.24463868	3.84921680	H	-4.51697067	-0.46189337	-1.11669748
H	-4.10154705	-0.03503745	3.09748641	C	1.26446576	0.04986296	-2.57960742
H	-0.19146809	0.36577562	4.71656694	C	1.26446576	0.04986296	2.57960742
H	-2.61818824	0.33154610	5.05089931	C	1.80514348	1.36150286	-3.21230064
C	-1.08313558	-0.03290111	-1.41665398	H	1.50340292	2.22600340	-2.61079288
C	-2.20353000	0.21878435	-4.05183676	H	1.42932355	1.50912231	-4.22913968
C	-2.49832001	-0.09753637	-1.65924598	H	2.89806798	1.35174068	-3.26347804
C	-0.26273159	0.09808153	-2.57677879	C	1.68642514	-1.16934263	-3.44526548
C	-0.83213987	0.24463868	-3.84921680	H	2.77441623	-1.24361924	-3.52984304
C	-3.02422187	0.02146763	-2.96060323	H	1.28324951	-1.10125257	-4.45983511
H	-0.19146809	0.36577562	-4.71656694	H	1.31782014	-2.09869405	-2.99732186
H	-4.10154705	-0.03503745	-3.09748641	C	1.68642514	-1.16934263	3.44526548
H	-2.61818824	0.33154610	-5.05089931	H	1.28324951	-1.10125257	4.45983511
C	1.17813083	-0.05772408	0.00000000	H	2.77441623	-1.24361924	3.52984304
C	4.00569355	-0.26243821	0.00000000	H	1.31782014	-2.09869405	2.99732186
C	1.91288366	-0.08537713	-1.21190305	C	1.80514348	1.36150286	3.21230064
C	1.91288366	-0.08537713	1.21190305	H	1.50340292	2.22600340	2.61079288
C	3.30747044	-0.19462906	1.19543384	H	2.89806798	1.35174068	3.26347804
C	3.30747044	-0.19462906	-1.19543384	H	1.42932355	1.50912231	4.22913968

Table S5. Cartesian Coordinates of **t-2**

atom	*x*	*y*	*z*	atom	*x*	*y*	*z*
B	0.00000000	0.00000000	-0.35129514	C	0.12064618	-1.21436557	1.92733199
C	-0.30998343	-0.60245296	-3.46369453	C	-0.12064618	1.21436557	1.92733199
C	0.30998343	0.60245296	-3.46369453	C	-0.12196981	1.20010164	3.32511317
H	-0.53181894	-0.99386422	-4.45679970	C	0.12196981	-1.20010164	3.32511317
H	0.53181894	0.99386422	-4.45679970	H	-0.21181404	2.11733389	3.89623939
C	0.28433288	1.36985531	-1.03176145	H	0.21181404	-2.11733389	3.89623939
C	1.46267459	3.77213175	-1.96599828	H	0.00000000	0.00000000	5.10487173
C	0.63888725	1.53068728	-2.40414458	C	-0.34922853	2.51871850	1.16383600
C	0.36793566	2.52083986	-0.19123621	C	0.34922853	-2.51871850	1.16383600
C	0.97992968	3.68357910	-0.65668012	C	1.87416517	-2.60714483	0.85514796

C	1.25014504	2.72707063	-2.84098816	H	2.44557956	-2.62330256	1.79082736
H	1.09467739	4.54676844	-0.01145286	H	2.20880906	-1.74998675	0.26345079
H	1.54168261	2.82123394	-3.88499732	H	2.09699181	-3.52172792	0.29230621
H	1.96131838	4.67915139	-2.30047775	C	0.00000000	-3.75290262	2.00989604
C	-0.28433288	-1.36985531	-1.03176145	H	0.60082425	-3.78000672	2.92282906
C	-1.46267459	-3.77213175	-1.96599828	H	0.23992873	-4.67442360	1.47098482
C	-0.36793566	-2.52083986	-0.19123621	H	-1.05839717	-3.77778889	2.29394889
C	-0.63888725	-1.53068728	-2.40414458	C	-1.87416517	2.60714483	0.85514796
C	-1.25014504	-2.72707063	-2.84098816	H	-2.09699181	3.52172792	0.29230621
C	-0.97992968	-3.68357910	-0.65668012	H	-2.44557956	2.62330256	1.79082736
H	-1.54168261	-2.82123394	-3.88499732	H	-2.20880906	1.74998675	0.26345079
H	-1.09467739	-4.54676844	-0.01145286	C	0.00000000	3.75290262	2.00989604
H	-1.96131838	-4.67915139	-2.30047775	H	-0.23992873	4.67442360	1.47098482
C	0.00000000	0.00000000	1.21259446	H	1.05839717	3.77778889	2.29394889
C	0.00000000	0.00000000	4.01674287	H	-0.60082425	3.78000672	2.92282906

Table S6. Cartesian Coordinates of **1b**

atom	*x*	*y*	*z*	atom	*x*	*y*	*z*
B	0.00194979	-1.06698252	0.00000000	H	-2.35461468	3.08070968	0.00000000
C	0.03892712	-1.76289809	1.40162460	C	-2.63219187	0.38315524	0.00000000
C	0.09033956	-2.74440458	4.08077936	H	-2.36448419	-0.68374241	0.00000000
C	-0.01213353	-0.90945112	2.53143688	C	-3.46618654	0.63567873	-1.26413776
C	0.11891989	-3.16413526	1.66709296	H	-4.36330562	0.00394185	-1.26678201
C	0.14271217	-3.61697485	3.00735742	H	-2.89230911	0.41354844	-2.17047689
C	0.01160056	-1.36972236	3.84044544	H	-3.79493596	1.68066139	-1.32230653
H	-0.07318570	0.16110872	2.36078110	C	-3.46618654	0.63567873	1.26413776
H	0.20408114	-4.68745070	3.19367934	H	-4.36330562	0.00394185	1.26678201
H	-0.03048282	-0.66595511	4.66848333	H	-3.79493596	1.68066139	1.32230653
H	0.11057415	-3.12896873	5.09803921	H	-2.89230911	0.41354844	2.17047689
C	0.03892712	-1.76289809	-1.40162460	C	2.46634376	0.64874478	0.00000000
C	0.09033956	-2.74440458	-4.08077936	H	2.30883324	-0.43989821	0.00000000
C	0.11891989	-3.16413526	-1.66709296	C	3.27048405	0.98403508	-1.26414947
C	-0.01213353	-0.90945112	-2.53143688	H	3.49091995	2.05705016	-1.32319785
C	0.01160056	-1.36972236	-3.84044544	H	2.72257712	0.70376342	-2.17041184
C	0.14271217	-3.61697485	-3.00735742	H	4.22740993	0.44719887	-1.26600315
H	-0.07318570	0.16110872	-2.36078110	C	3.27048405	0.98403508	1.26414947
H	-0.03048282	-0.66595511	-4.66848333	H	3.49091995	2.05705016	1.32319785
H	0.20408114	-4.68745070	-3.19367934	H	4.22740993	0.44719887	1.26600315
H	0.11057415	-3.12896873	-5.09803921	H	2.72257712	0.70376342	2.17041184
C	0.18158289	-4.21849059	0.67794462	C	-0.32386642	4.88194867	0.00000000
C	0.18158289	-4.21849059	-0.67794462	H	-1.39338085	5.13728768	0.00000000
H	0.24003153	-5.21318354	1.12047650	C	0.29428663	5.49491771	-1.26480057
H	0.24003153	-5.21318354	-1.12047650	H	-0.16498087	5.08283293	-2.17054670
C	-0.08365659	0.52835952	0.00000000	H	1.37185773	5.29661806	-1.31736628
C	-0.23129410	3.36548603	0.00000000	H	0.15578676	6.58339552	-1.27574319

C	-1.33368543	1.18227816	0.00000000	C	0.29428663	5.49491771	1.26480057
C	1.09273313	1.31132451	0.00000000	H	-0.16498087	5.08283293	2.17054670
C	1.00187560	2.70637260	0.00000000	H	0.15578676	6.58339552	1.27574319
C	-1.38598580	2.58115493	0.00000000	H	1.37185773	5.29661806	1.31736628
H	1.91779390	3.29583057	0.00000000				

Table S7. .Cartesian Coordinates of **10**

atom	*x*	*y*	*z*	atom	*x*	*y*	*z*
B	-0.09400866	-0.00000006	-0.00005282	H	-0.50775257	3.28790424	-3.31236997
C	0.59272445	-0.9871437	0.99435282	H	3.5216512	2.25077551	-2.26703329
C	1.57459112	-2.87424108	2.89525186	H	1.95859464	3.59119365	-3.61760478
C	-0.2638721	-1.78310237	1.79598502	C	-1.68608452	-0.00000059	0.00000717
C	1.99688538	-1.17437632	1.18311852	C	-4.51825098	-0.00000271	0.00011508
C	2.44974518	-2.11872817	2.13437896	C	-2.41766685	0.8518359	-0.84560153
C	0.1973949	-2.70482487	2.72443737	C	-2.4175999	-0.85183721	0.84567072
H	-1.33618952	-1.66534851	1.67725681	C	-3.81377363	-0.8548058	0.84866985
H	3.52182369	-2.25033894	2.26708607	C	-3.81384015	0.85480229	-0.84849419
H	-0.50750054	-3.28822413	3.31197841	H	-1.8889063	1.52777189	-1.5166372
H	1.9588699	-3.59114117	3.61739519	H	-1.88878781	-1.52777257	1.51666628
C	0.59264879	0.98719333	-0.9944613	H	-4.35134533	-1.52622291	1.51521987
C	1.57437081	2.87429243	-2.89543334	H	-4.35146426	1.52621837	-1.51500301
C	1.99679536	1.17463954	-1.1831218	H	-5.60590904	-0.00000379	0.00015679
C	-0.26400876	1.78295655	-1.79622234	C	3.05211012	-0.47753628	0.48137759
C	0.19718758	2.70466783	-2.72472092	H	4.04862919	-0.78899394	0.79529851
C	2.44958279	2.11899267	-2.13441542	C	3.0520735	0.47804842	-0.48121405
H	-1.33631715	1.66505101	-1.67756308	H	4.04856869	0.78972345	-0.79499499

Table S8. Cartesian Coordinates of Radical Anion **p-2**$^{\bullet-}$

atom	*x*	*y*	*z*	atom	*x*	*y*	*z*
B	-0.40033182	-0.04670777	0.00000000	H	3.86898324	-0.15982894	-2.12683391
C	-1.08272260	-0.02101970	1.41683113	H	3.86898324	-0.15982894	2.12683391
C	-2.20796161	0.17708796	4.08756873	H	5.11193659	-0.26301319	0.00000000
C	-0.26879433	0.07331173	2.59310183	C	-3.53731976	-0.25022217	-0.67315363
C	-2.50153329	-0.07051292	1.67862904	C	-3.53731976	-0.25022217	0.67315363
C	-3.02590859	0.02797321	2.97560732	H	-4.52692158	-0.39433118	-1.11237349
C	-0.83603670	0.18417126	3.87084036	H	-4.52692158	-0.39433118	1.11237349
H	-4.10743020	-0.01434776	3.10405048	C	1.26624294	0.03645539	2.58963163
H	-0.18638703	0.27014200	4.73860794	C	1.26624294	0.03645539	-2.58963163
H	-2.62107280	0.26593361	5.09067041	C	1.70942881	-1.19207783	3.43009739
C	-1.08272260	-0.02101970	-1.41683113	H	1.30935373	-1.15192862	4.44935248
C	-2.20796161	0.17708796	-4.08756873	H	2.80060323	-1.25972875	3.50367592
C	-2.50153329	-0.07051292	-1.67862904	H	1.34518184	-2.11352407	2.96161758
C	-0.26879433	0.07331173	-2.59310183	C	1.79377707	1.33839811	3.25182915
C	-0.83603670	0.18417126	-3.87084036	H	1.41219077	1.46432009	4.27142914

C	-3.02590859	0.02797321	-2.97560732	H	1.47928439	2.20811894	2.66369977
H	-0.18638703	0.27014200	-4.73860794	H	2.88861619	1.34386257	3.30157343
H	-4.10743020	-0.01434776	-3.10405048	C	1.70942881	-1.19207783	-3.43009739
H	-2.62107280	0.26593361	-5.09067041	H	1.30935373	-1.15192862	-4.44935248
C	1.16226851	-0.05165237	0.00000000	H	1.34518184	-2.11352407	-2.96161758
C	4.02492365	-0.19819539	0.00000000	H	2.80060323	-1.25972875	-3.50367592
C	1.91624216	-0.06749491	1.21012395	C	1.79377707	1.33839811	-3.25182915
C	1.91624216	-0.06749491	-1.21012395	H	1.47928439	2.20811894	-2.66369977
C	3.31139973	-0.14621491	-1.19262272	H	1.41219077	1.46432009	-4.27142914
C	3.31139973	-0.14621491	1.19262272	H	2.88861619	1.34386257	-3.30157343

Table S9. Cartesian Coordinates of Radical Anion **t-2**$^{\bullet-}$

atom	*x*	*y*	*z*	atom	*x*	*y*	*z*
B	0.00000000	0.00000000	-0.35312993	C	0.07944931	-1.21753178	1.93336774
C	-0.30373833	-0.60501696	-3.45911155	C	-0.07944931	1.21753178	1.93336774
C	0.30373833	0.60501696	-3.45911155	C	-0.05600467	1.20448917	3.32998791
H	-0.50916590	-0.99910441	-4.45761670	C	0.05600467	-1.20448917	3.32998791
H	0.50916590	0.99910441	-4.45761670	H	-0.09603251	2.13014826	3.89764884
C	0.32676859	1.36030217	-1.02323936	H	0.09603251	-2.13014826	3.89764884
C	1.53840010	3.77461816	-1.95750552	H	0.00000000	0.00000000	5.12186418
C	0.66062881	1.54543632	-2.40349268	C	-0.31502792	2.51820602	1.15856411
C	0.42578065	2.52078919	-0.18644434	C	0.31502792	-2.51820602	1.15856411
C	1.06635421	3.67411535	-0.64497619	C	1.83541365	-2.58239995	0.83037164
C	1.27630340	2.73036763	-2.83890792	H	2.42283283	-2.58766737	1.75847141
H	1.19942759	4.52841289	0.01261710	H	2.13604533	-1.71459195	0.23536871
H	1.54265543	2.82889003	-3.89179696	H	2.06497237	-3.49169449	0.25832327
H	2.04858036	4.67580517	-2.29363810	C	0.00000000	-3.76267807	2.00140084
C	-0.32676859	-1.36030217	-1.02323936	H	0.61864275	-3.78524460	2.90465110
C	-1.53840010	-3.77461816	-1.95750552	H	0.23608541	-4.67715976	1.44604065
C	-0.42578065	-2.52078919	-0.18644434	H	-1.05331146	-3.80200078	2.30632842
C	-0.66062881	-1.54543632	-2.40349268	C	-1.83541365	2.58239995	0.83037164
C	-1.27630340	-2.73036763	-2.83890792	H	-2.06497237	3.49169449	0.25832327
C	-1.06635421	-3.67411535	-0.64497619	H	-2.42283283	2.58766737	1.75847141
H	-1.54265543	-2.82889003	-3.89179696	H	-2.13604533	1.71459195	0.23536871
H	-1.19942759	-4.52841289	0.01261710	C	0.00000000	3.76267807	2.00140084
H	-2.04858036	-4.67580517	-2.29363810	H	-0.23608541	4.67715976	1.44604065
C	0.00000000	0.00000000	1.20265211	H	1.05331146	3.80200078	2.30632842
C	0.00000000	0.00000000	4.03248355	H	-0.61864275	3.78524460	2.90465110

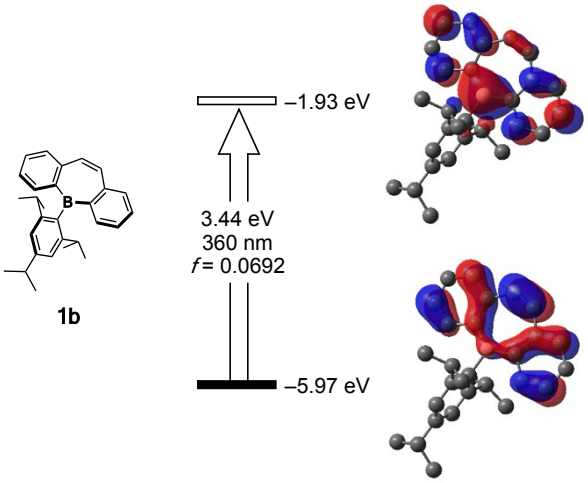

Figure S10. Energy diagrams and Kohn–Sham plots of HOMO and LUMO for **1b** calculated at the TD-B3LYP/6-31+G(d) level of theory.

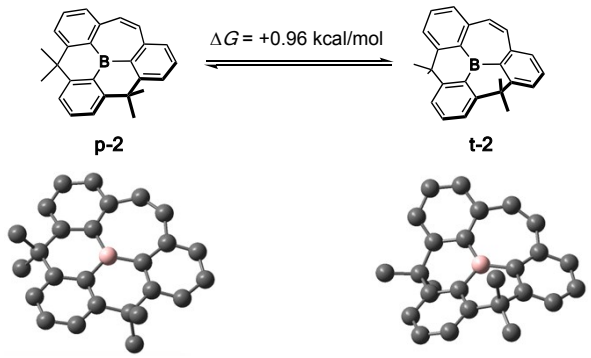

Figure S11. Optimized structures for **p-2** and **t-2** and the energy difference (*ΔG*) in the ground state calculated at the B3PW91/6-31+G(d) level of theory.

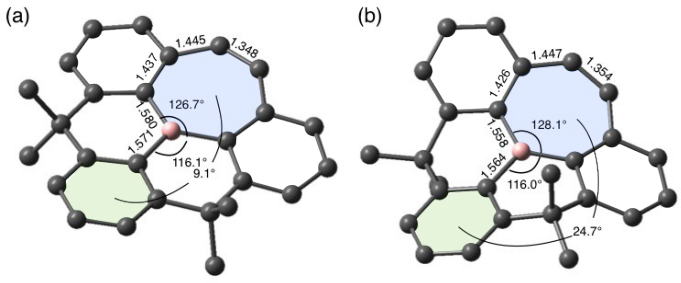

Figure S12. Selected bond lengths (Å) and angles (°) in the optimized structures of (a) **p-2** and (b) **t-2**.

Table S10. Energy Differences (*ΔG*) between **p-2** and **t-2** in the Ground State

	p-2 / a.u.	**t-2** / a.u.	*ΔG* / kcal·mol^{-1}
B3PW91/6-31+G(d)	-1028.774051	-1028.774051	0.96
B3PW91/6-31+G(d,p)	-1028.807278	-1028.805721	0.98
CAMB3LYP/6-31+G(d)	-1028.548925	-1028.547045	1.18
M06-2X/6-31+G(d)	-1028.725555	-1028.724137	0.89
PBE0/def2SVP	-1027.193491	-1027.190585	1.82

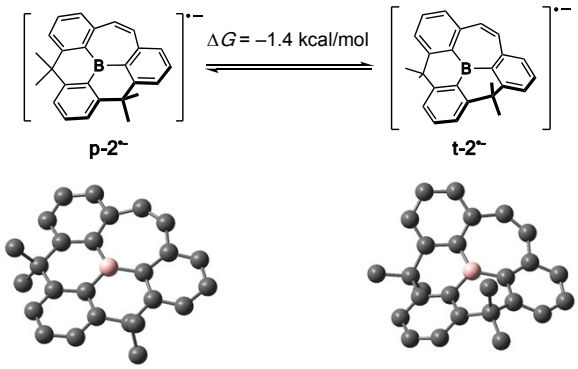

Figure S13. Optimized structures for the radical anions **p-2**$^{\bullet-}$ and **t-2**$^{\bullet-}$ and the energy difference (*ΔG*) in the ground state calculated at the UB3PW91/6-31+G(d) level of theory.

7. References

1 Z. Zhou, A. Wakamiya, T. Kushida and S. Yamaguchi, *J. Am. Chem. Soc*., 2012, **134**, 4529.

2 A. Shuto, T. Kushida, T. Fukushima, H. Kaji and S. Yamaguchi, *Org. Lett.*, 2013, **15**, 6234.

3 L. G. Mercier, W. E. Piers and M. Parvez, *Angew. Chem*., 2009, **121**, 6224; *Angew. Chem., Int. Ed*., 2009, **48**, 6108.

4 A. Pelter, K. Smith, D. Buss and Z. Jin, *Heteroatom Chem.*, 1992, **3**, 275.

5 G. M. Sheldrick, *SHELXL-2017/1, Program for the Refinement of Crystal Structures*; University of Göttingen: Göttingen, Germany, 2017.

6 S. Solé and F. P. Gabbaï, *Chem. Commun*., 2004, 1284.

7 J. Frisch, G. W. Trucks, H. B. Schlegel, G. E. Scuseria, M. A. Robb, J. R. Cheeseman, G. Scalmani, V. Barone, G. A. Petersson, H. Nakatsuji, X. Li, M. Caricato, A. V. Marenich, J. Bloino, B. G. Janesko, R. Gomperts, B. Mennucci, H. P. Hratchian, J. V. Ortiz, A. F. Izmaylov, J. L. Sonnenberg, D. Williams-Young, F. Ding, F. Lipparini, F. Egidi, J. Goings, B. Peng, A. Petrone, T. Henderson, D. Ranasinghe, V. G. Zakrzewski, J. Gao, N. Rega, G. Zheng, W. Liang, M. Hada, M. Ehara, K. Toyota, R. Fukuda, J. Hasegawa, M. Ishida, T. Nakajima, Y. Honda, O. Kitao, H. Nakai, T. Vreven, K. Throssell, J. A. Montgomery, Jr., J. E. Peralta, F. Ogliaro, M. J. Bearpark, J. J. Heyd, E. N. Brothers, K. N. Kudin, V. N. Staroverov, T. A. Keith, R. Kobayashi, J. Normand, K. Raghavachari, A. P. Rendell, J. C. Burant, S. S. Iyengar, J. Tomasi, M. Cossi, J. M. Millam, M. Klene, C. Adamo, R. Cammi, J. W. Ochterski, R. L. Martin, K. Morokuma, O. Farkas, J. B. Foresman, and D. J. Fox, *Gaussian 16, Revision A.03*, Gaussian, Inc., Wallingford CT, 2016.

8 T. Kushida, Z. Zhou, A.Wakamiya and S. Yamaguchi, *Chem. Commun.*, 2012, **48**, 10715.

8. NMR Spectra

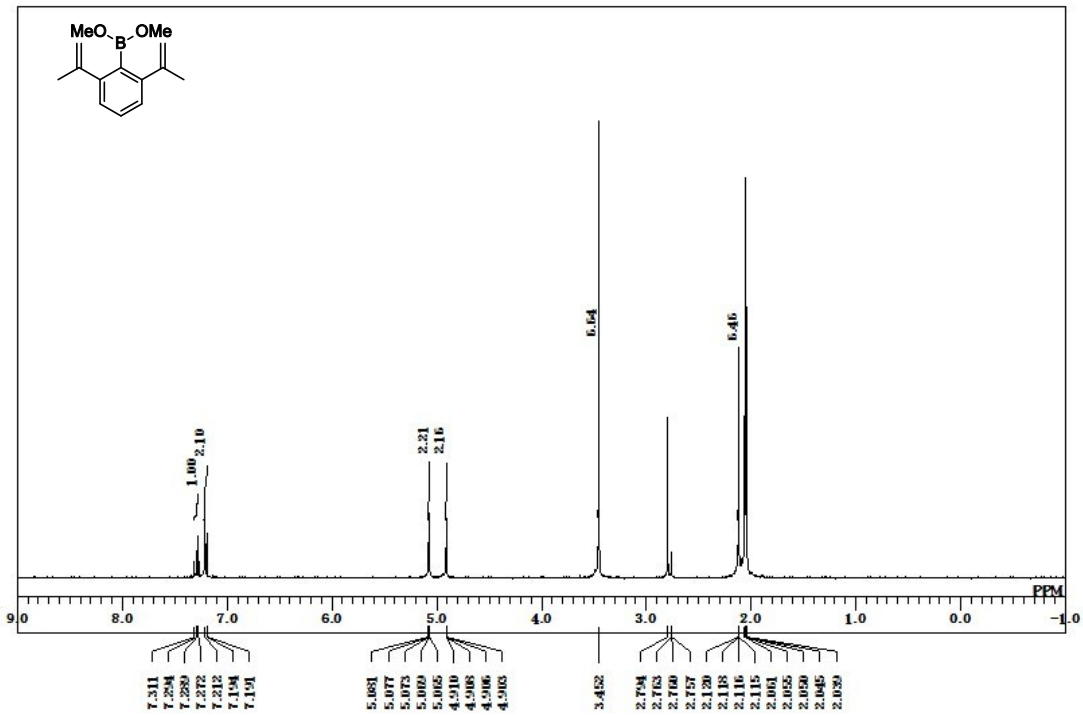

Figure S14. ^{1}H NMR spectrum of **S1** (400 MHz, acetone-d_6).

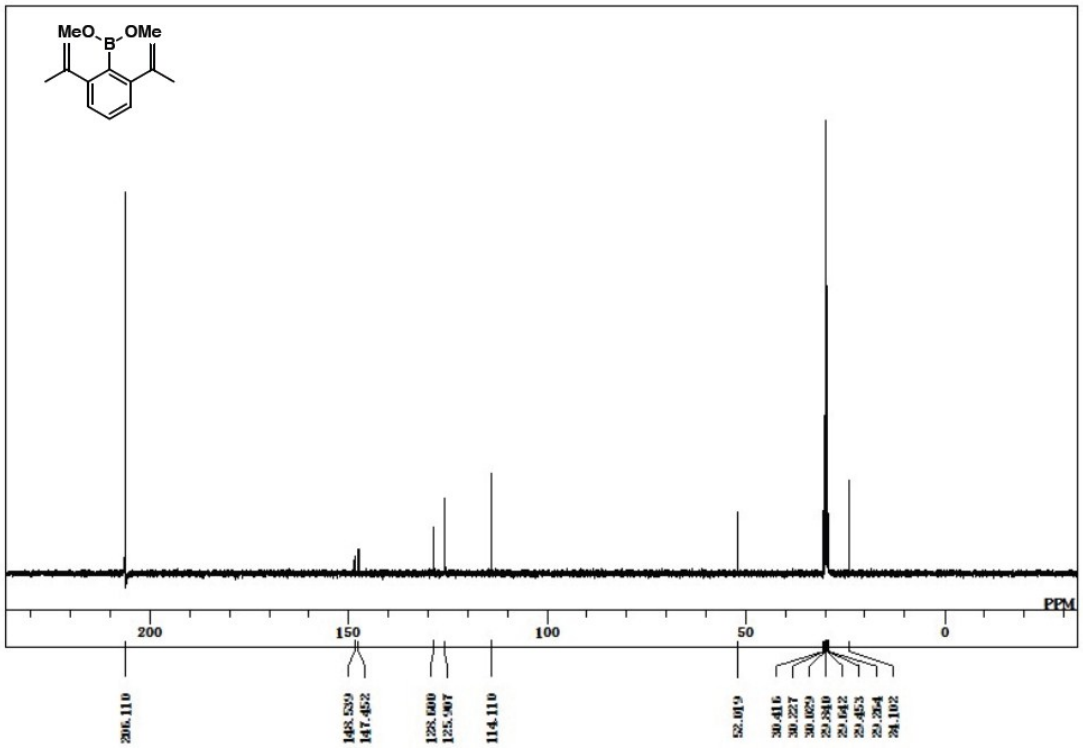

Figure S15. $^{13}C\{^{1}H\}$ NMR spectrum of **S1** (100 MHz, acetone-d_6).

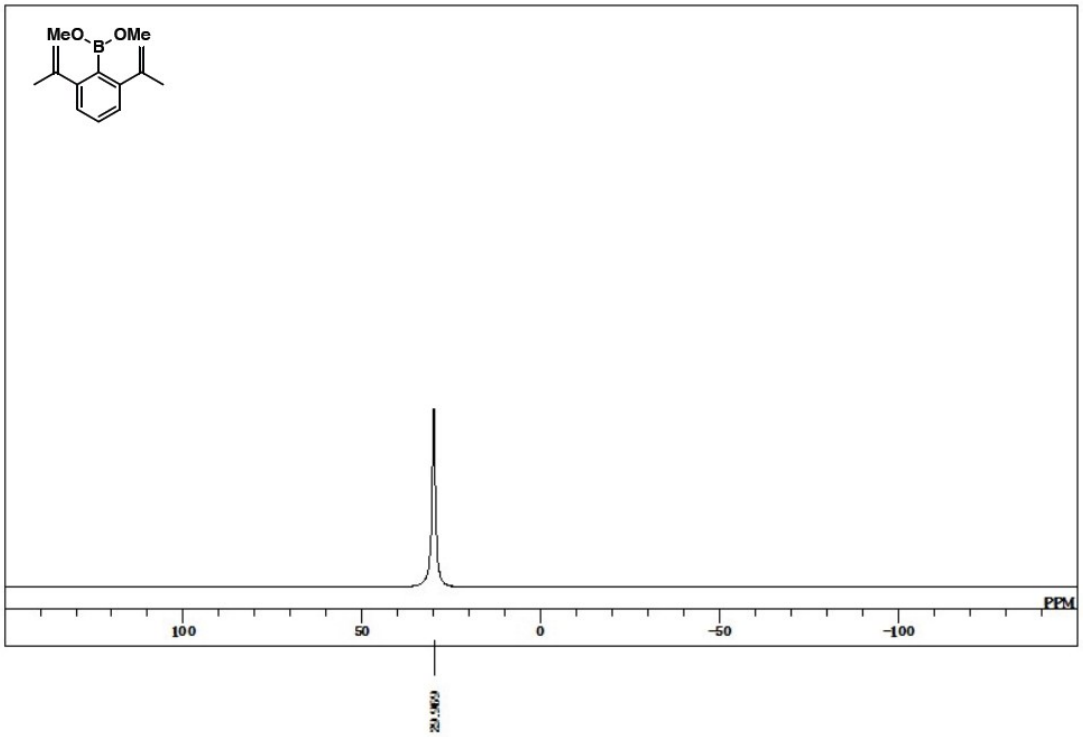

Figure S16. $^{11}B\{^{1}H\}$ NMR spectrum of **S1** (128 MHz, acetone-d_6).

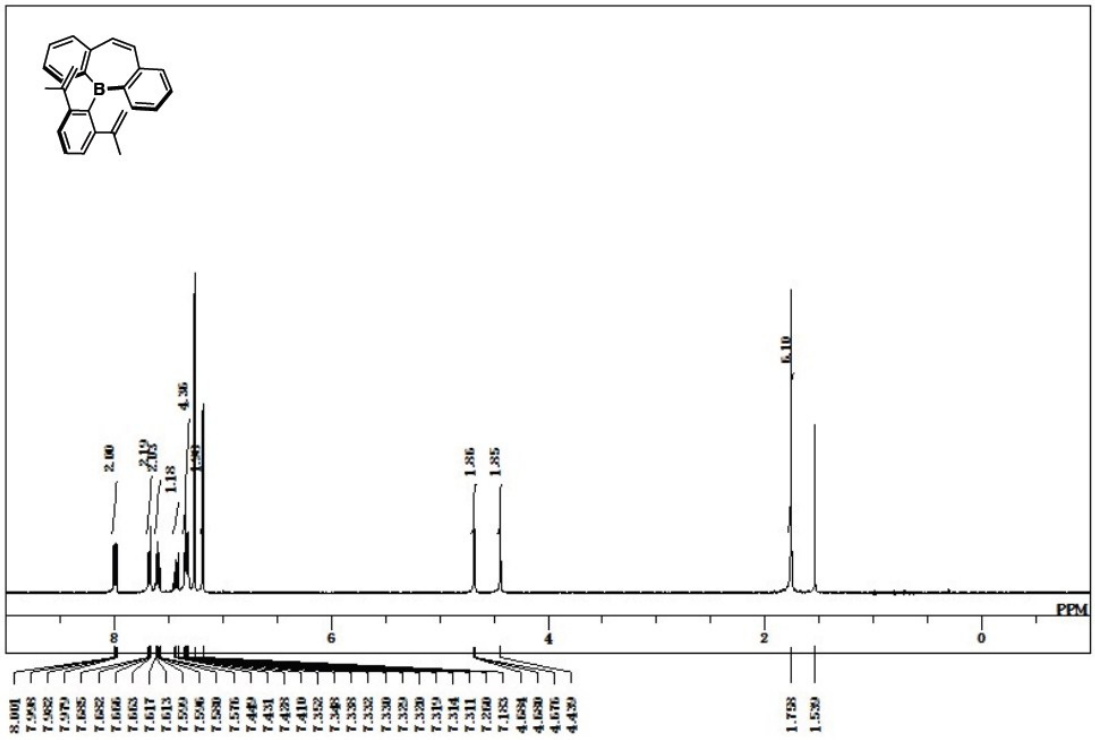

Figure S17. ^{1}H NMR spectrum of **6** (400 MHz, $CDCl_3$).

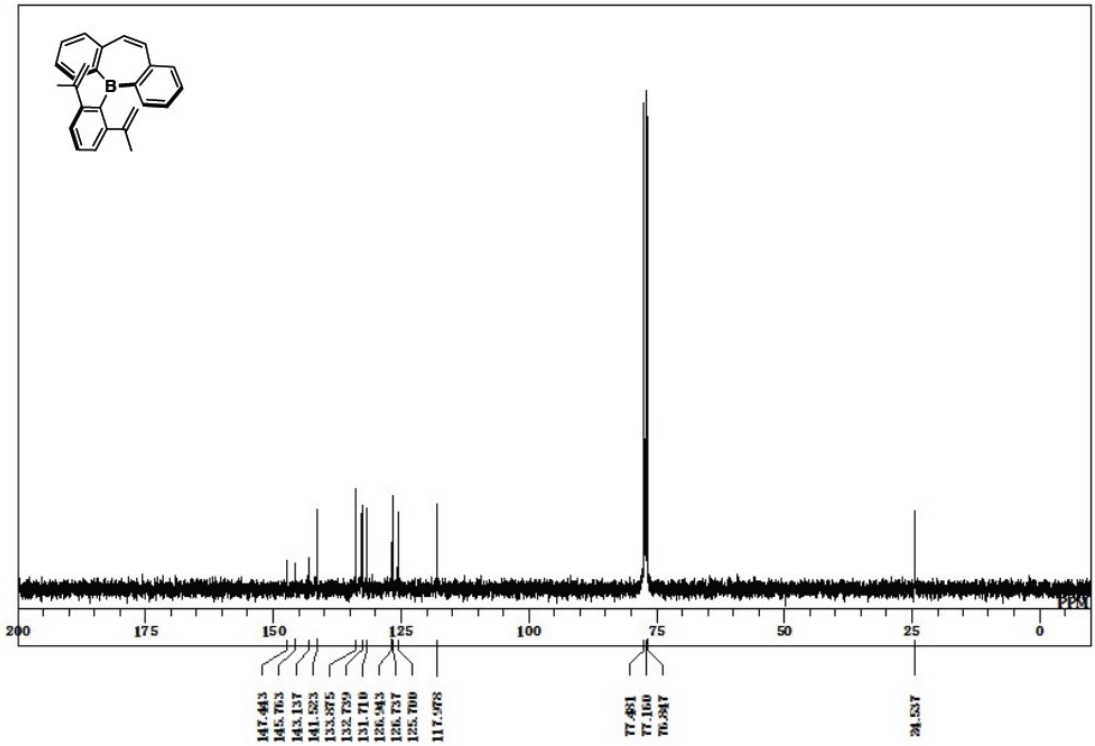

Figure S18. $^{13}C\{^{1}H\}$ NMR spectrum of **6** (100 MHz, $CDCl_3$).

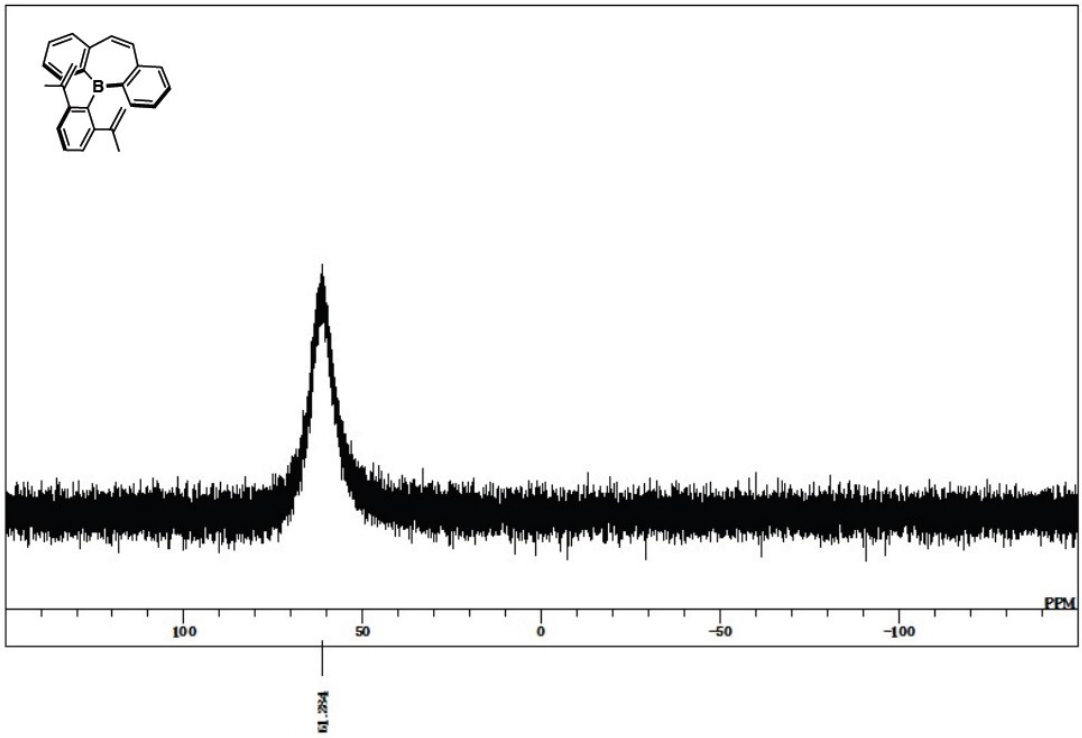

Figure S19. $^{11}B\{^{1}H\}$ NMR spectrum of **6** (128 MHz, $CDCl_3$).

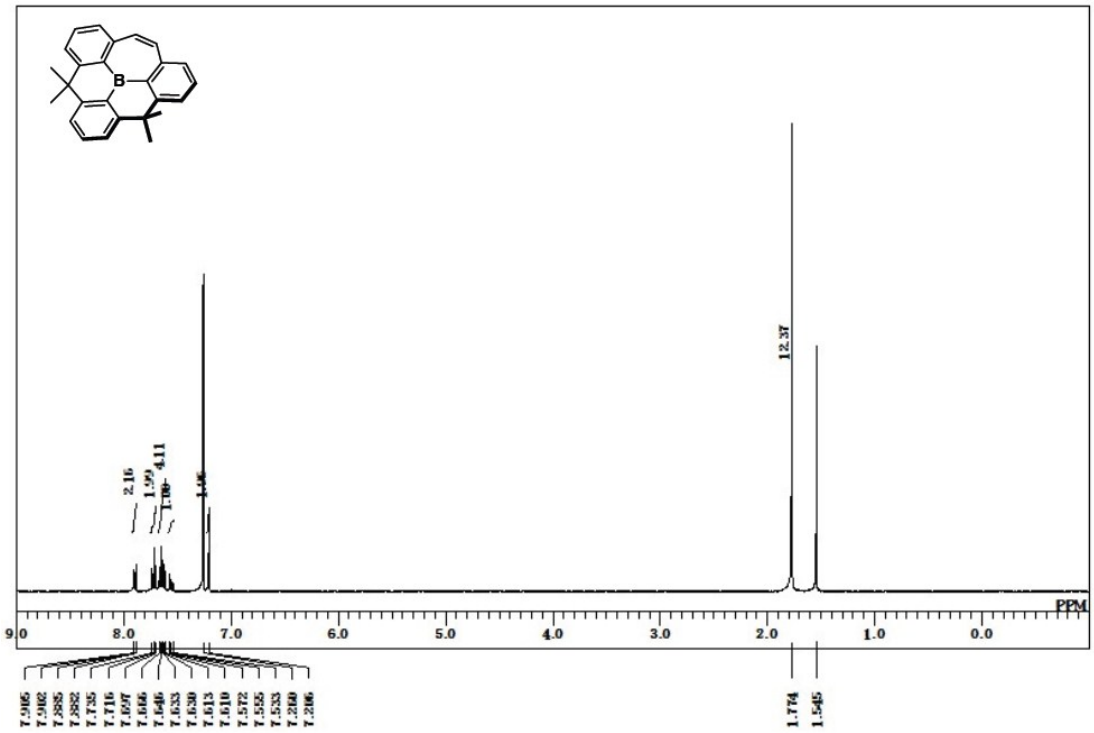

Figure S20. ^{1}H NMR spectrum of **2** (400 MHz, $CDCl_3$).

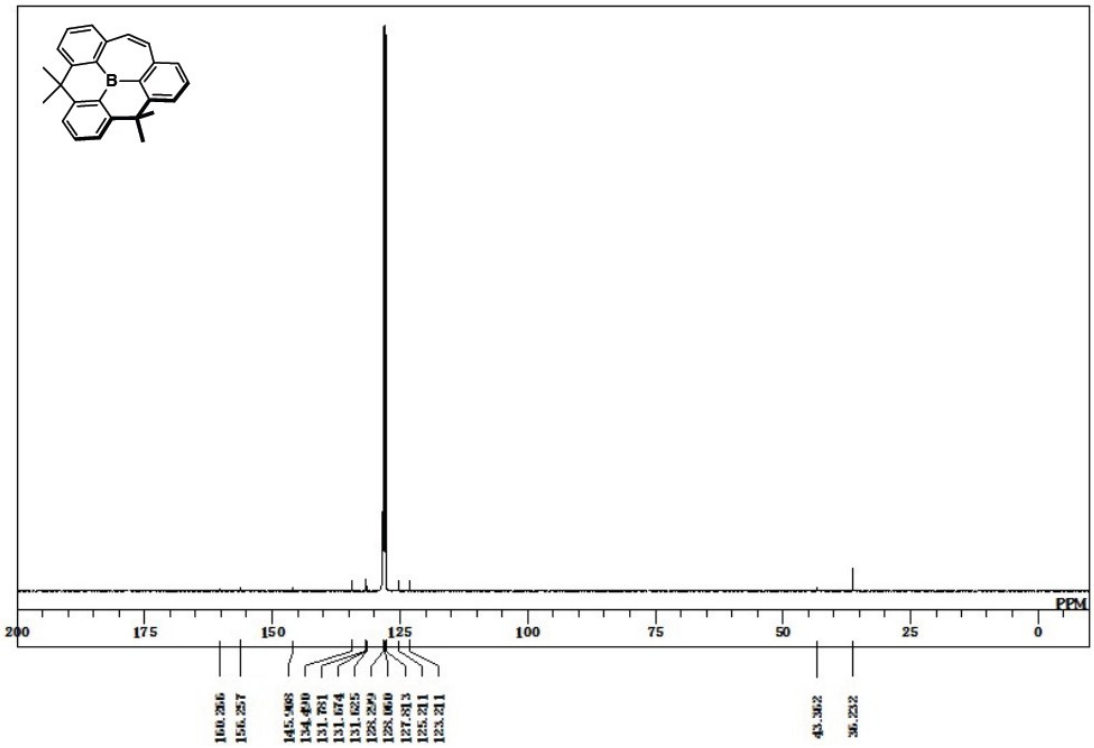

Figure S21. $^{13}C\{^{1}H\}$ NMR spectrum of **2** (100 MHz, C_6D_6).

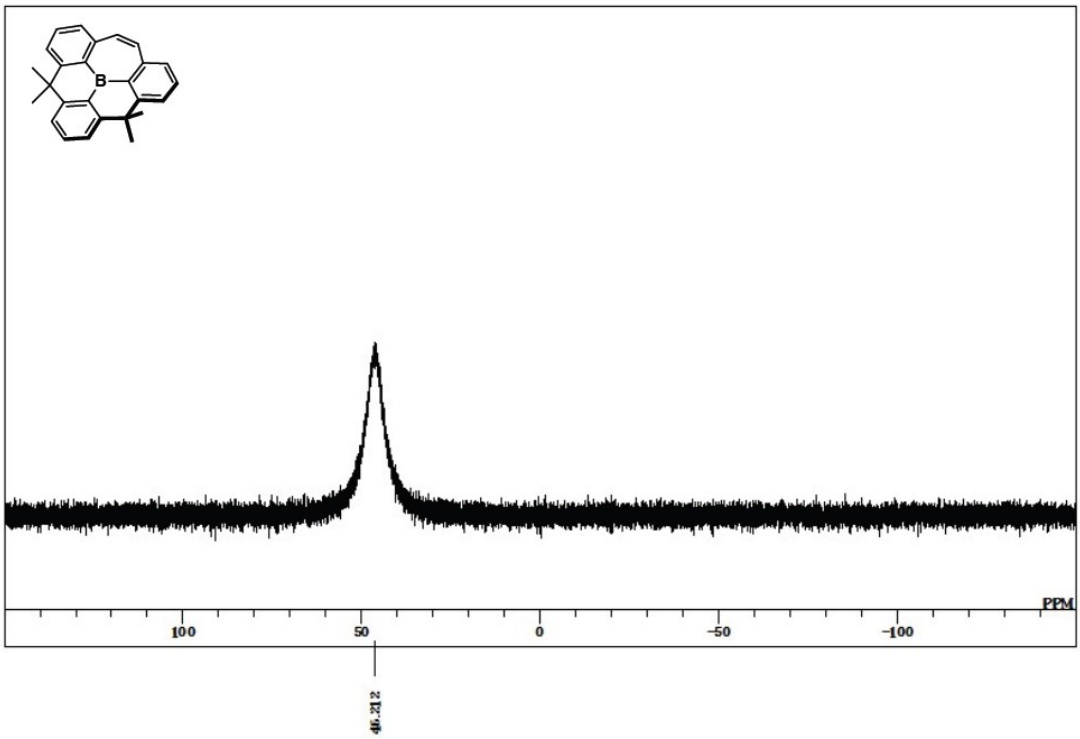

Figure S22. $^{11}B\{^{1}H\}$ NMR spectrum of **2** (128 MHz, $CDCl_3$).

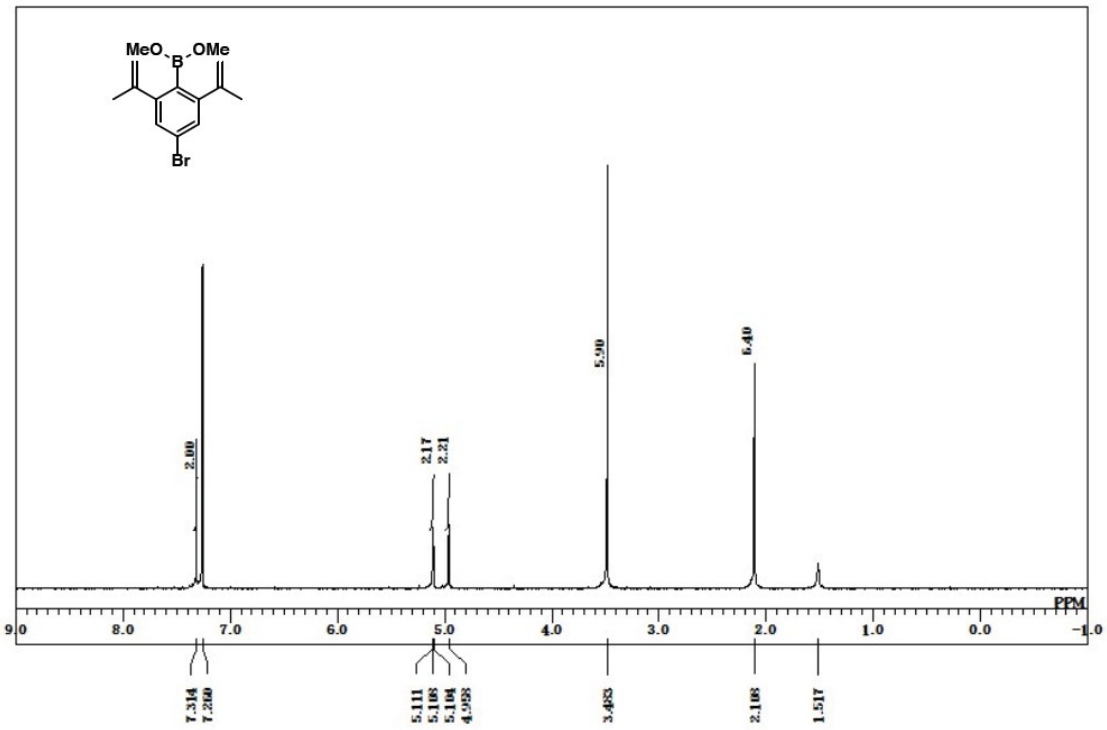

Figure S23. ^{1}H NMR spectrum of **S2** (400 MHz, $CDCl_3$).

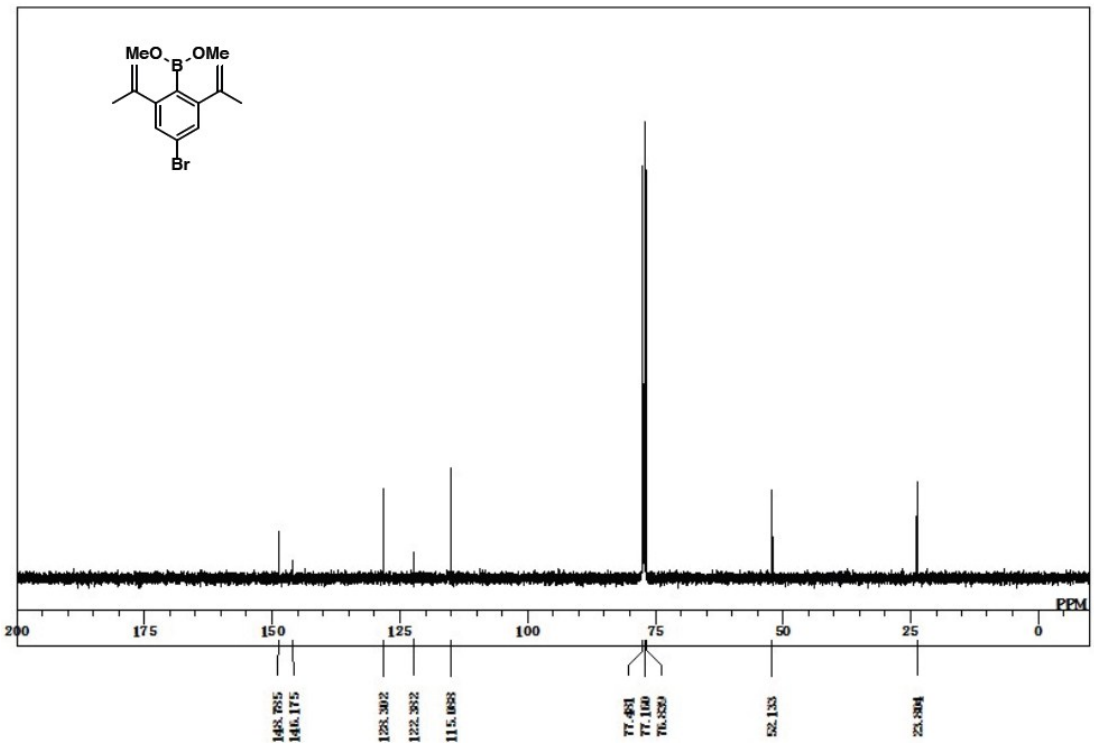

Figure S24. ^{13}C{^{1}H} NMR spectrum of **S2** (100 MHz, $CDCl_3$).

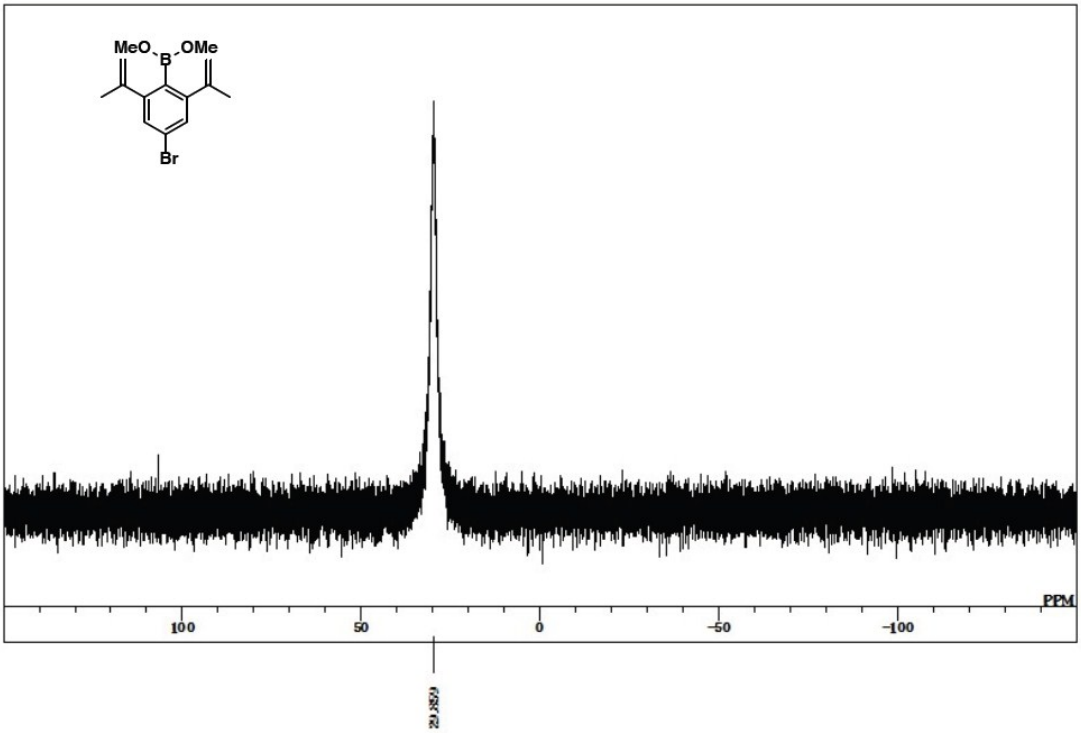

Figure S25. $^{11}B\{^{1}H\}$ NMR spectrum of **S2** (128 MHz, $CDCl_3$).

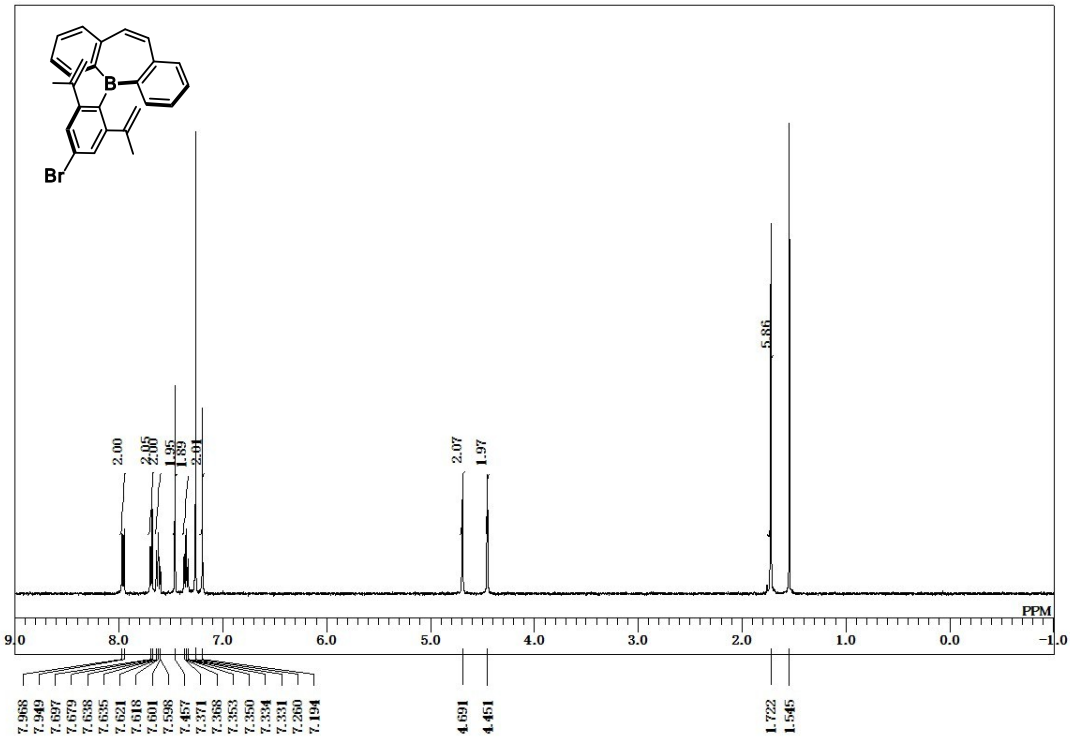

Figure S26. ^{1}H NMR spectrum of **7** (400 MHz, $CDCl_3$).

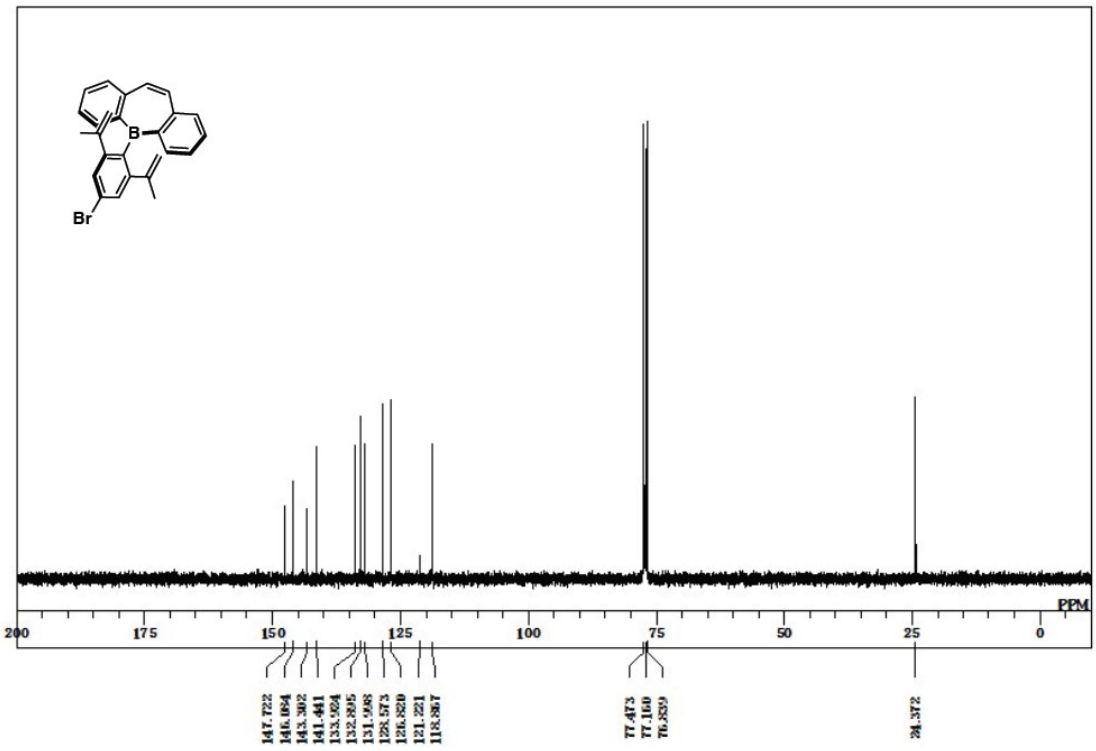

Figure S27. $^{13}C\{^{1}H\}$ NMR spectrum of **7** (100 MHz, $CDCl_3$).

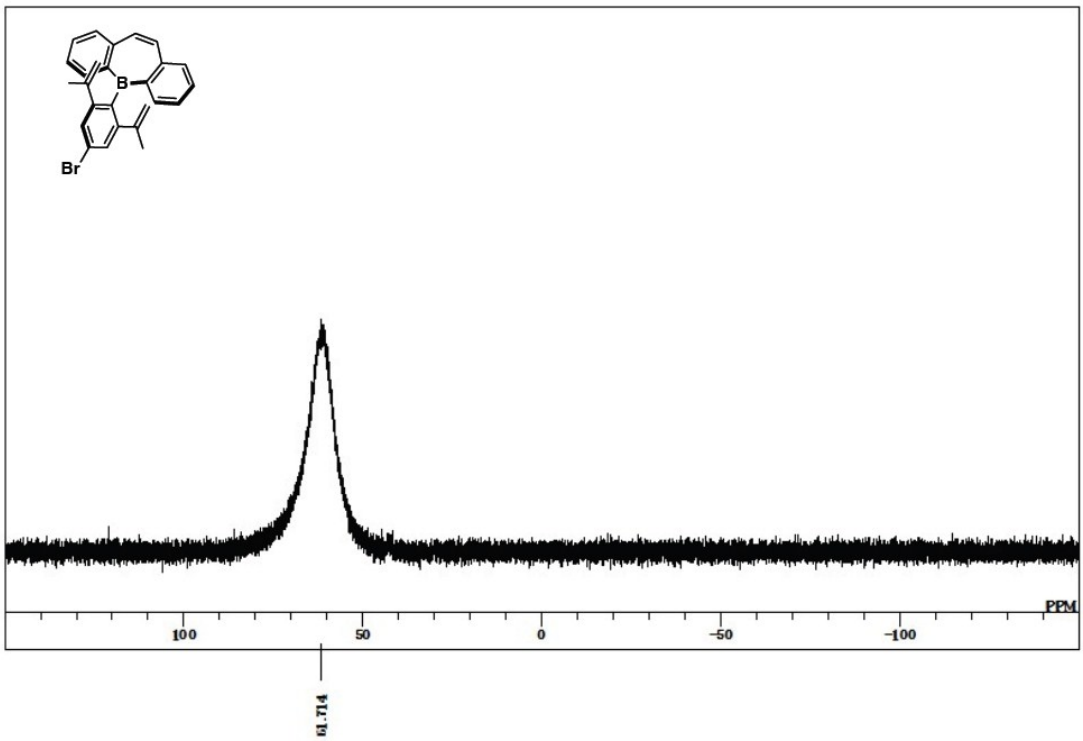

Figure S28. $^{11}B\{^{1}H\}$ NMR spectrum of **7** (128 MHz, $CDCl_3$).

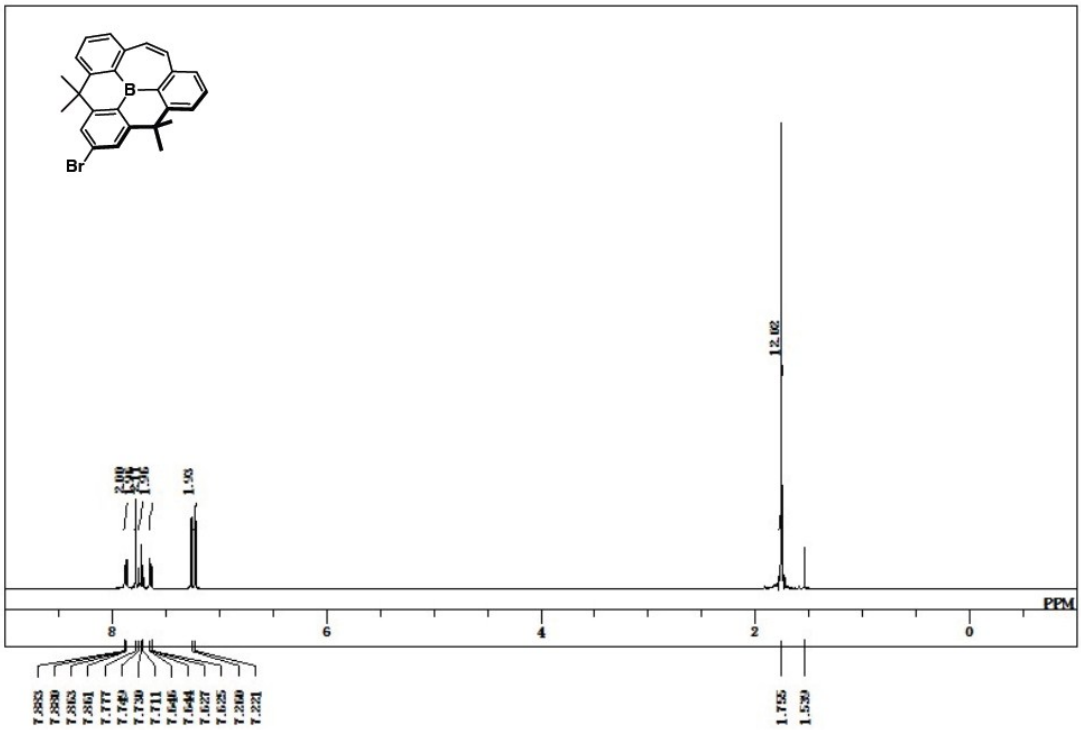

Figure S29. ^{1}H NMR spectrum of **8** (400 MHz, $CDCl_3$).

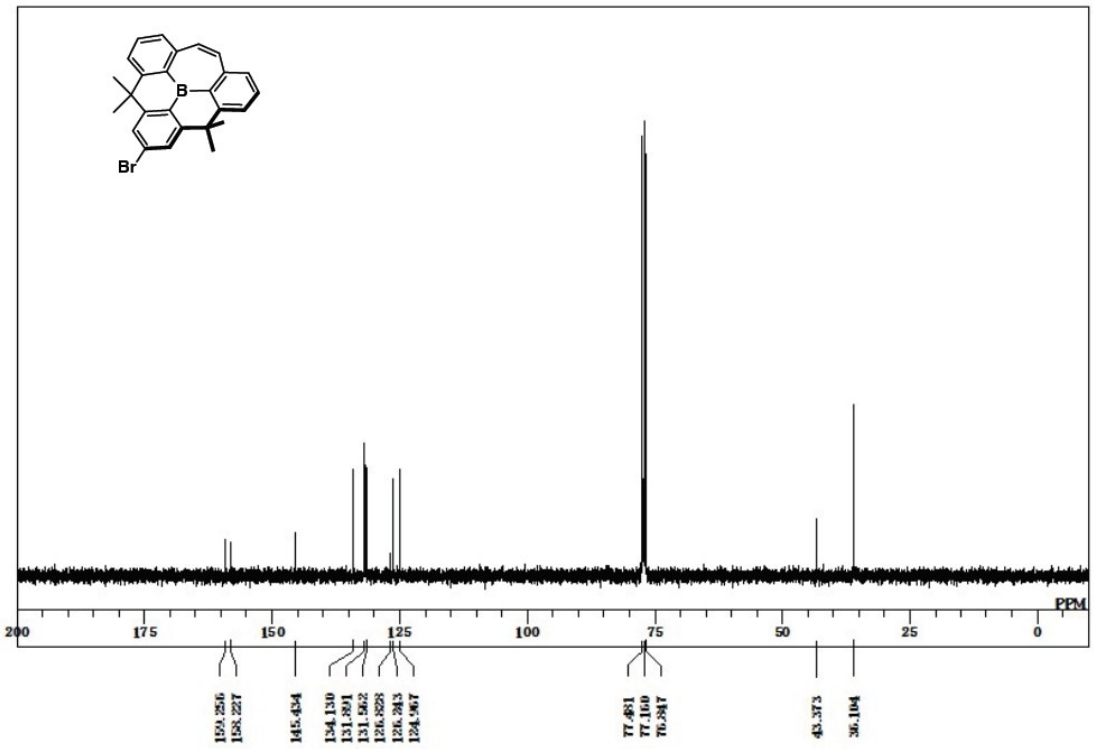

Figure S30. ^{13}C{^{1}H} NMR spectrum of **8** (100 MHz, $CDCl_3$).

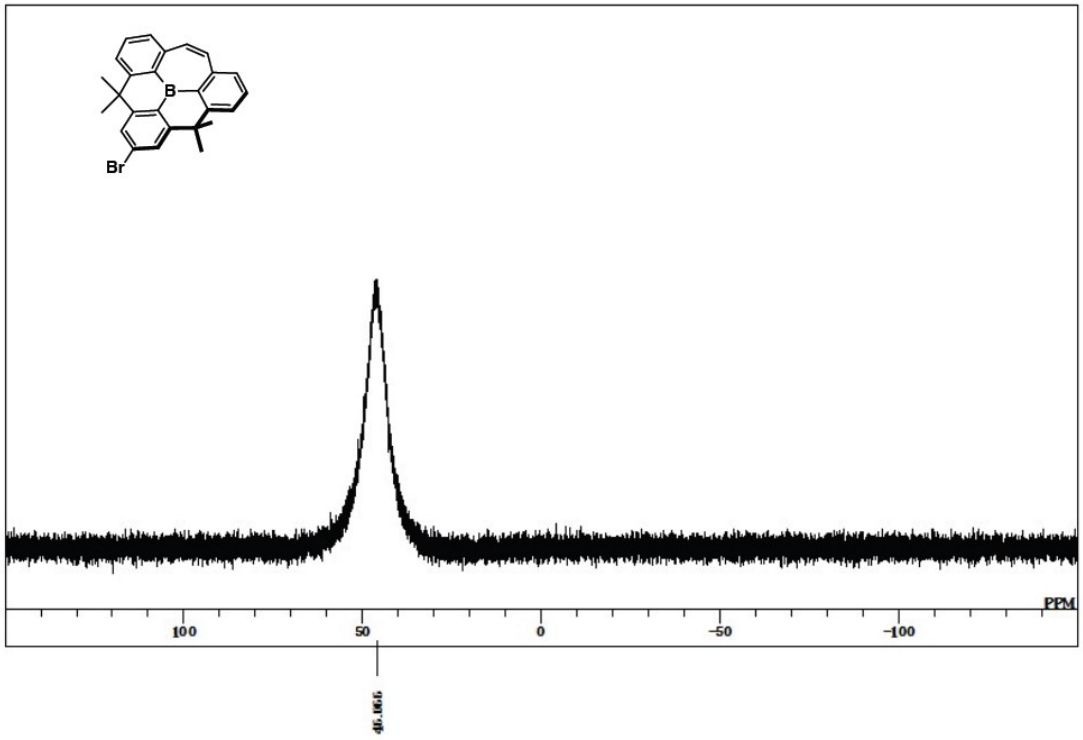

Figure S31. $^{11}B\{^{1}H\}$ NMR spectrum of **8** (128 MHz, $CDCl_3$).

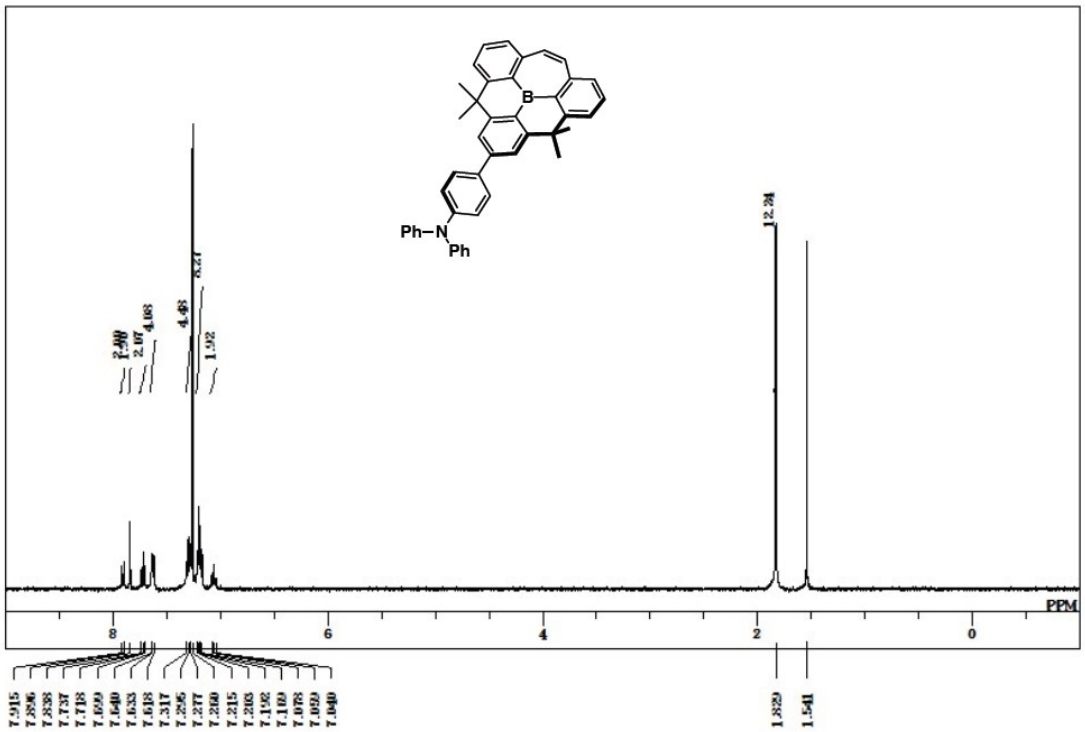

Figure S32. ^{1}H NMR spectrum of **9** (400 MHz, $CDCl_3$).

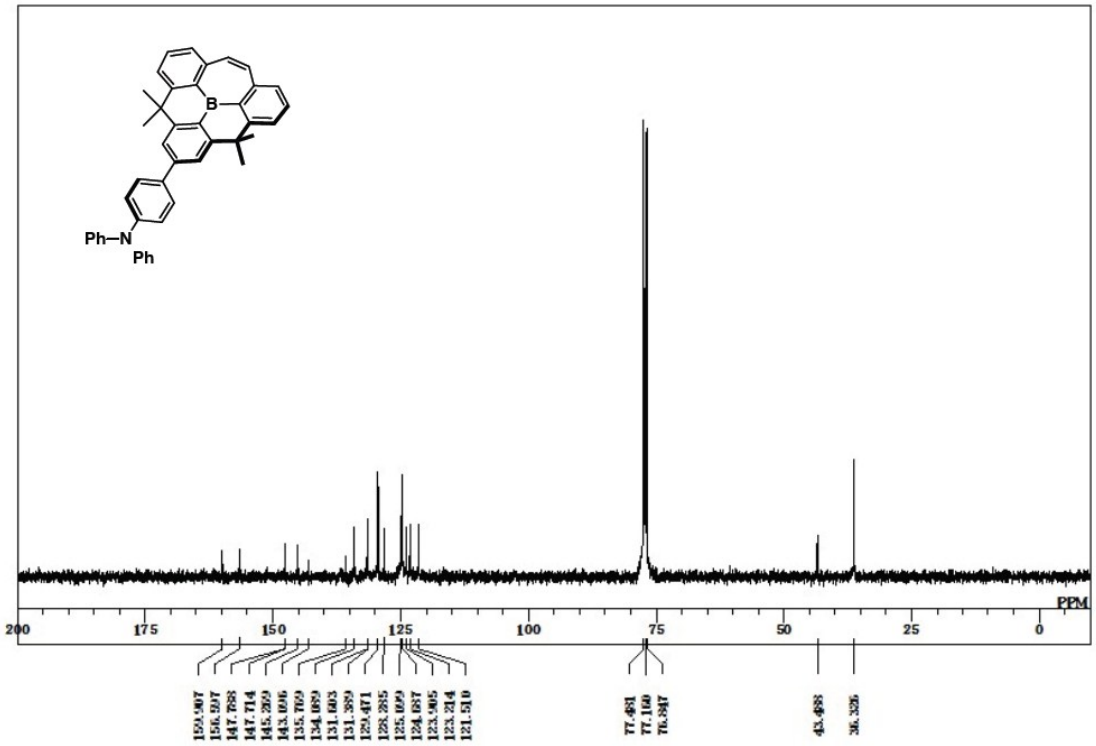

Figure S33. $^{13}C\{^{1}H\}$ NMR spectrum of **9** (100 MHz, $CDCl_3$).

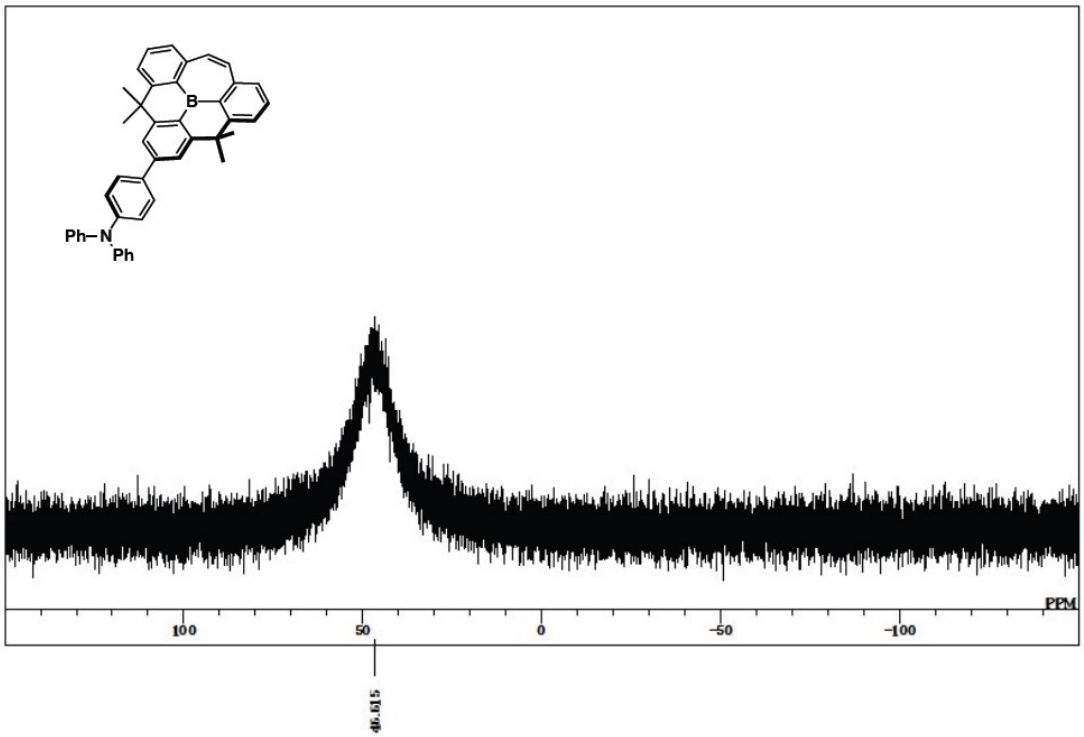

Figure S34. $^{11}B\{^{1}H\}$ NMR spectrum of **9** (128 MHz, $CDCl_3$).

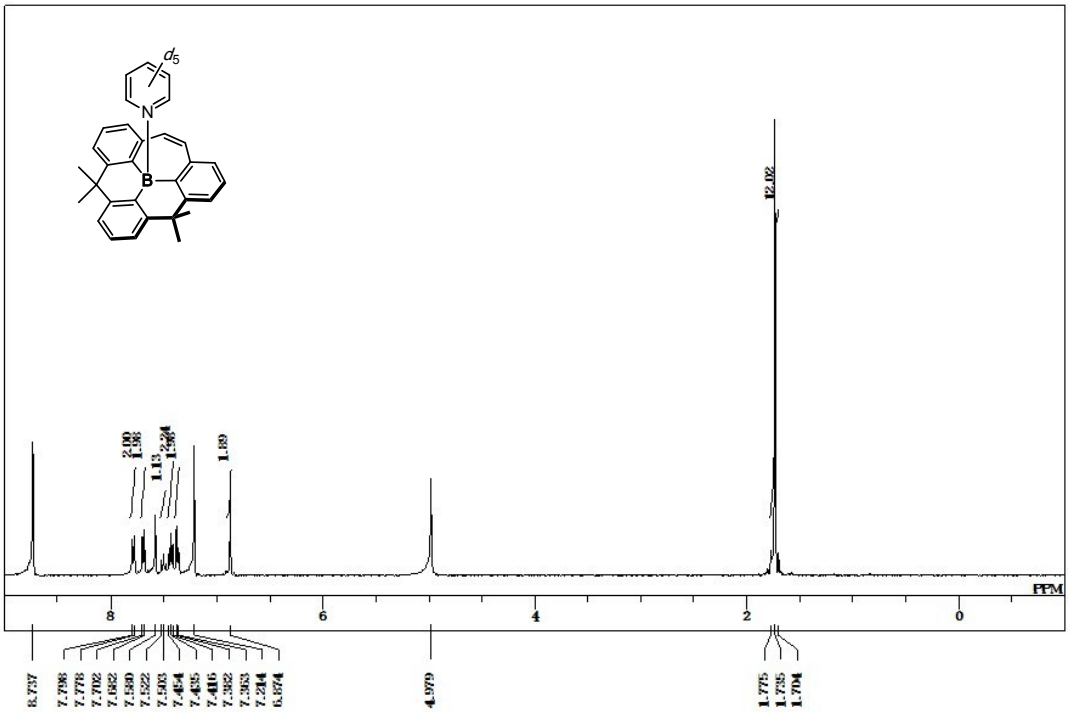

Figure S35. ^{1}H NMR spectrum of **2**·Py (400 MHz, pyridine-d_5).

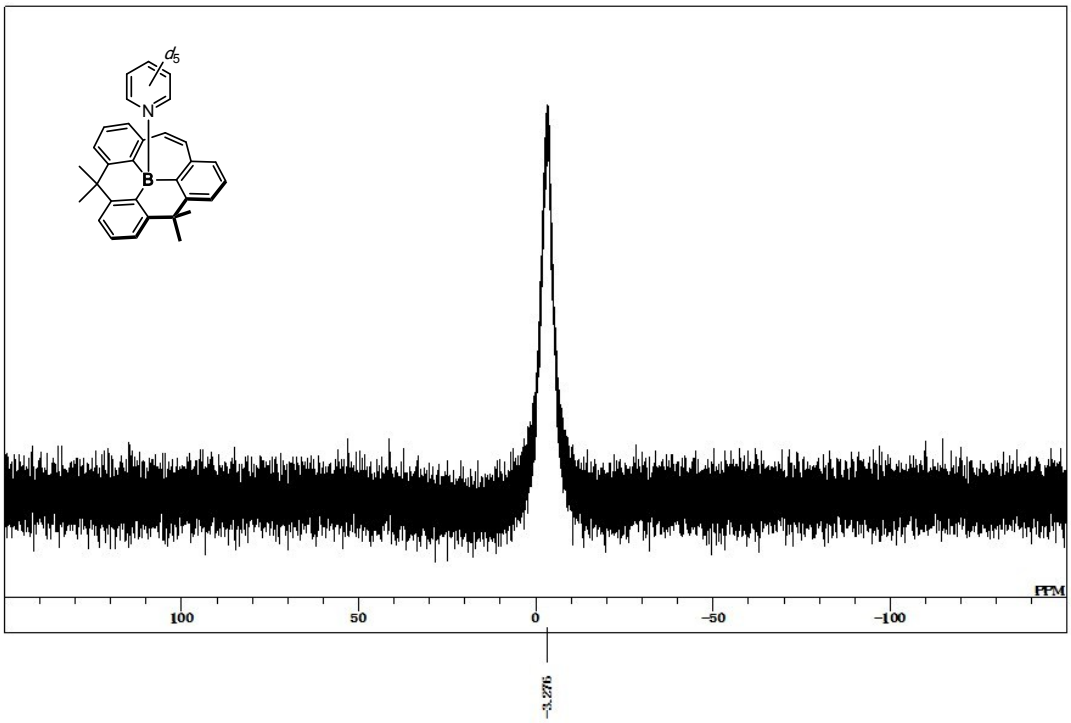

Figure S36. ^{11}B{^{1}H} NMR spectrum of **2**·Py (128 MHz, pyridine-d_5).

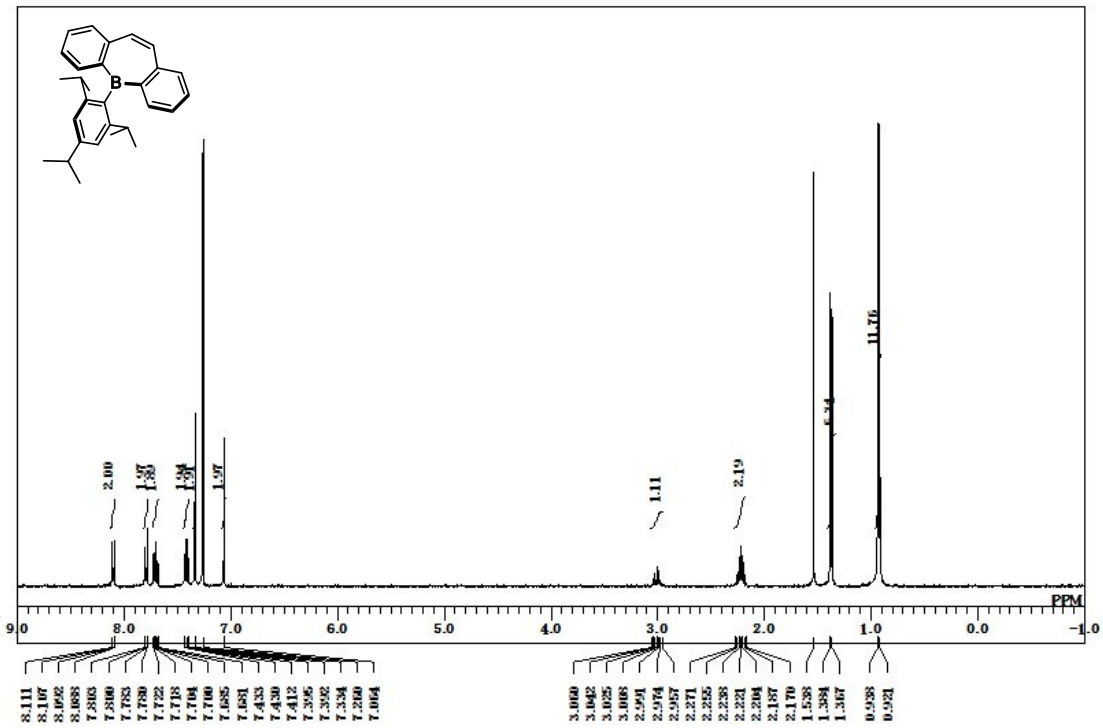

Figure S37. ^{1}H NMR spectrum of **1b** (400 MHz, $CDCl_3$).

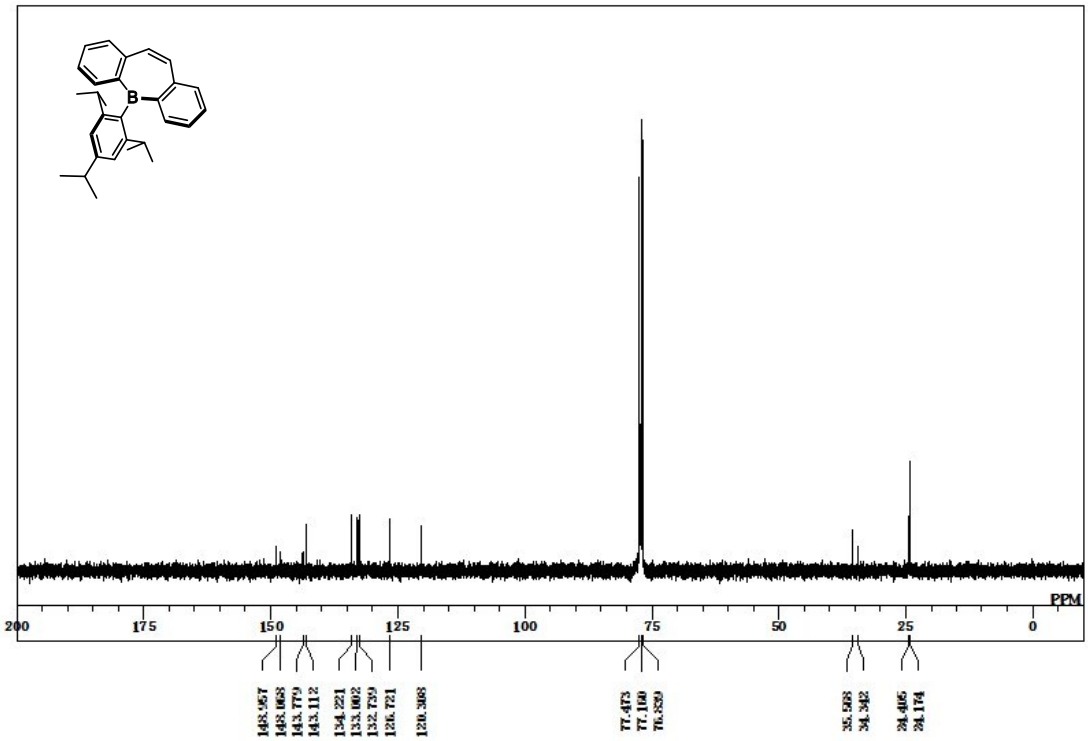

Figure S38. $^{13}C\{^{1}H\}$ NMR spectrum of **1b** (100 MHz, $CDCl_3$).

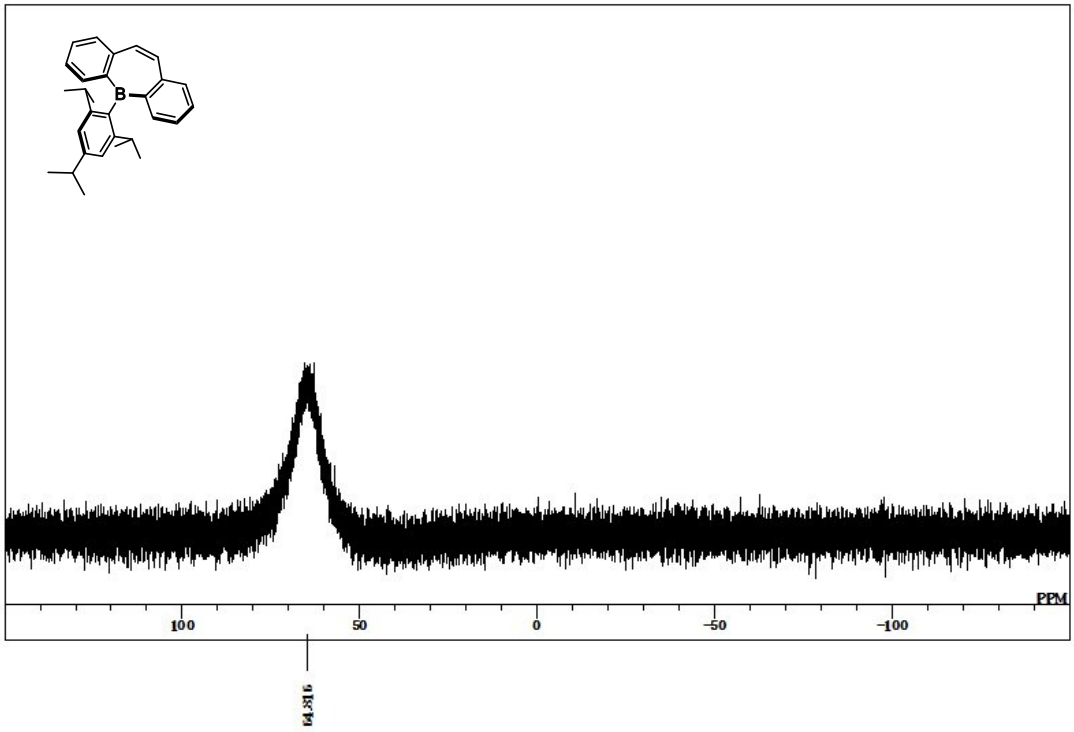

Figure S39. $^{11}B\{^{1}H\}$ NMR spectrum of **1b** (128 MHz, $CDCl_3$).

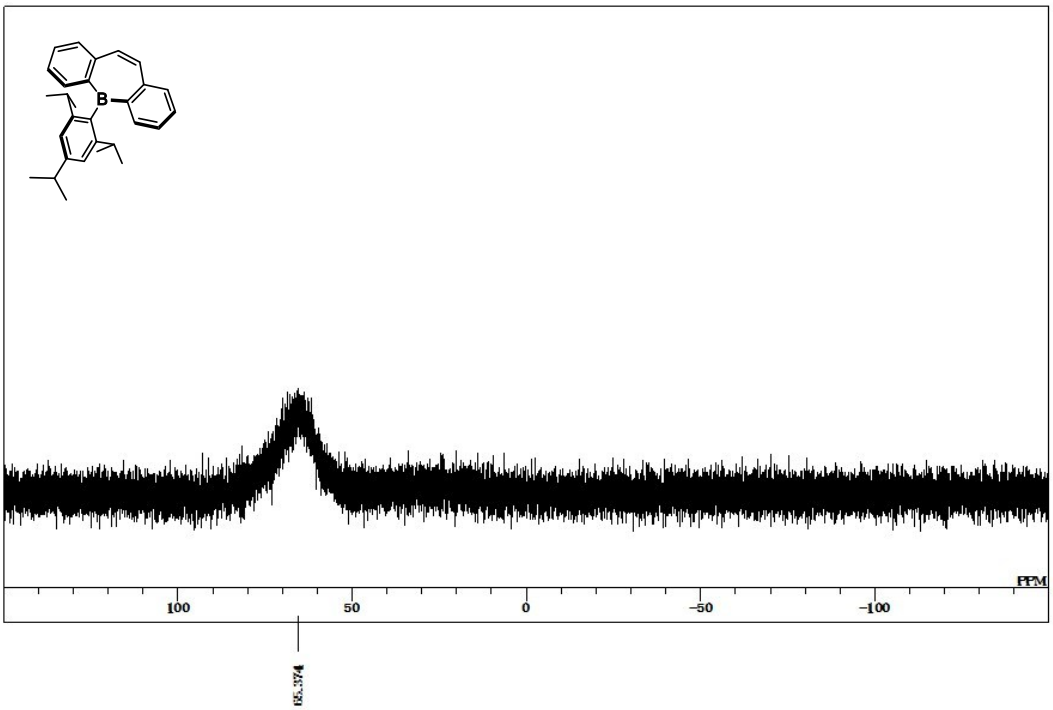

Figure S40. $^{11}B\{^{1}H\}$ NMR spectrum of **1b** (128 MHz, pyridine-d_5).